ALMA MATER STUDIORUM
UNIVERSITÀ DI BOLOGNA

SCHOOL OF ENGINEERING AND ARCHITECTURE

Forlì Campus

Second Cycle Degree in
AEROSPACE ENGINEERING
Class LM-20

THESIS

in Applied Aerodynamics

Characterization of Flow Structures During Continuous Valve Opening Testing for Swirl Number Evaluation in Diesel Engine Cylinder

CANDIDATE
Chiara Olivieri

SUPERVISOR
Prof. P. Henrik Alfredsson

ASSISTANT SUPERVISOR
Dr.Eng. Björn Lindgren

EXAMINER
Prof. Gian Marco Bianchi

Academic Year 2015/2016
Session II

Abstract

As world trucks (busses and industrial diesel engines) producer, Scania AB needs to respect international regulation about pollution and to develop competitive products.

To accomplish these goals the engines production needs to respect the design and the tolerances given by the development department. One of the main parameter to be controlled is the Swirl Number, the ratio between the angular momentum and the axial momentum of the flow inside the cylinder. Nowadays the Swirl evaluation test is performed on few sample cylinder heads with stationary test at the central laboratory at the Scania Technical Center in Sweden. Considering both the test mean time (25 minutes) and the time required to bring the cylinder heads from the production sites to the laboratory, in case of error Scania will suffer large economic losses.

The aim of this work was to reduce the test time needed to perform experimental test to evaluate the Swirl Number and the Flow Coefficient. The time reduction was obtained investigating a continuous way to perform the evaluation test. Experimental tests show that continuous tests to evaluate the Swirl Number are possible. With the set up used in this work the test time was 10 minutes, saving the 65% of the original time.

Acknowledgements

Foremost, I would like to express my sincere gratitude to my thesis advisor Professor P. Henrik Alfredsson for his patience and motivation. His guidance helped me in the time of research and writing of this thesis. His precious teaching will guide me in my future works.

Besides my advisor, I would like to thank Dr.Eng. Björn Lindgren, my supervisor at Scania and my thesis co-advisor. He was always supportive whenever I ran into a trouble spot or had a question about my research or writing.

I would like to thank Jonas Holmborn for allowing me to participate to this project, and all the NMGP staff at Scania for welcoming me in the office.

Thanks to Bastian and Tommy that with their helps and suggestions easier my staying in Sweden.

A huge thank to Fredrik and the lab technicians Jim and Timo, without their help the experimental part of this project would have been very difficult. Thanks to Timo that overcoming the language barrier managed to help me in the $R\&D$ test bench, and a special thanks to Jim, for the help in all the experimental phases and for the very long chats that made the waiting time enjoyable.

My sincere thanks to Professor Alessandro Talamelli: for being able to share his enthusiasm about Aerodynamics, for being able to motivate me, for teaching me how to love this wonderful subject and for having suggested Professor P. Henrik Alfredsson as advisor during my master thesis in Scania.

I cannot forget my amazing friends in Forlì. Antonio, Caterina and Sandhya, wonderful friends that shared with me the amazing years of the master. Dalila, that was always there for me, whatever the case. Giulia and Oscar, that shared with me incredible summers of study. And finally Lorenzo and Otavio my two favourite crazy people, without them it would not be as fun as it was. Thank you guys for these years

and the crazy adventures that we made together, each of you made my journey wonderful and easier.

Thanks to my incredible flatmates, Benedetta, Lucrezia and Marzia, for have shared a small part of our life together, for the insane evenings and for the mad afternoon of study.

I would love to thank Laura, that is by my side since high school. Thank you for your patience with my lunatic mood, for the tons of moments and events shared together and for the support shown during my master thesis experience.

Thank you to Giulia, a very special friend. Thanks for always be there for me, for sharing countless of new experiences with me. Without you never would have been the same and I would have not loved this journey. Thank you.

I would also like to thank my sister Sara and my "auntie" Paola, they even came to Stockholm to share a part of this experience with me (probably they will not do anything similar again since the amount of kilometers per day that I imposed them).

Thank you to my grandmother Flavia, her lucky shoes on the door for each exam were always useful.

Finally, I must express my very profound gratitude to my mother Cecilia and to Roberto. They made this journey possible and they are always there when I need to reach for help. None of this would have been possible without they huge support. Thank you for everything.

My more sincere thank you to all of you

Chiara

Contents

List of Symbols

Symbol	Definition	Dimension
A_0	Intake valve area	mm^2
A_{cyl}	Cylinder cross section area	mm^2
$AT01$	Bypass valve position	V
$AT02$	Intake valves position	mm
BP	Bypass position	V
$BT01VEL$	Bypass valve velocity	—
$BT02VEL$	Intake valves velocity	—
c_m	Mean piston velocity	m/s
$c(\alpha)$	Instantaneous piston velocity	m/s
c	Piston speed	m/s
d_0	Intake valve inner seat diameter	mm
d_l	Laser beam diameter	mm
D	Cylinder inner diameter	mm
d_0	Intake valve seat diameter	mm
dz	Piston velocity	m/s
EA	Ensemble average	—
f_D	Doppler frequency	Hz
FFT	Fast Fourier Transform	—
$\dot{I}$	Angular momentum flux	Nm
i	i^{th} cycle	—
L	Intake valves lift	mm
LDA	Laser Doppler Anemometry	—
LDV	Laser Doppler Velocimetry	—
M	Torque	Nm
$\dot{m}$	Mass time derivative or mass flow	kg/s
$ML00$	Torque at the honeycomb	Nmm
n_D	Paddle wheel speed	rpm
n	Fictitious engine speed	rpm (Hz for AVL)
n	Number of intake valves	—
N	Swirl Number	—
$NL00$	Flow meter velocity	rmp
p	Pressure	Pa or as specified
PDF	Probability Density Function	—
$PL00$	Ambient pressure	mbar
$PL01$	Pressure drop over the flow meter	Pa

$PL02$	Pressure drop over the cylinder	Pa
q_{eff}	Effective mass flow	kg/s
q_{theo}	Theoretical mass flow	kg/s
q_v	Volume flow	m^3/s
R^2	Coefficient of determination	—
R	Crank	mm
R	Gas constant	J/kg K
R	Cylinder radius	mm
r	Radial distance from the cylinder axis	mm
SNR	Signal to Noise Ratio	—
s	Stroke	mm
T	Air temperature	K
TDC	top dead center	—
$TL01$	Temperature after the flow meter	C
$TL02$	Temperature after the cylinder	C
u_x	horizontal velocity component	m/s
U	Generic flow velocity	m/s
$\overline{U}$	Mean velocity	m/s
u	Turbulent fluctuation	m/s
$UT01$	Engine control variable	V
V_r	Radial velocity	m/s
V_s	Stroke volume	mm^3
V_t	Tangential velocity	m/s
V_z	Axial velocity at cylinder axis	m/s
$V(r)$	Tangential velocity function of the radius	m/s
V	Cylinder volume	mm^3
VL	Valve lifter velocity	—
w_m	Mean flow velocity	m/s
w	Flow velocity	m/s
y	Distance form piston TDC position	mm
z	Instantaneous displacement over stroke volume	—
α	Intake valve seat angle	rad
α	Crank Angle	deg
β	Area Ratio	—
Δp	Pressure difference	Pa
δ_f	Fringe distance	μm
γ	Heat capacity ratio c_p/c_v	—
λ	Wavelength	

$\mu\sigma$	Flow Coefficient	—
ω	Angular velocity	rad/s
ρ	Density	kg/m^3
θ	Laser beams angle	deg

Chapter 1

Introduction

Scania AB is a Swedish automotive company specialized in heavy-duty trucks and buses but also designs diesel engine for industrial purposes. Scania designs trucks with a gross vehicle weight rating up to more than 16 tons, trucks that can be used for long-distance haulage, construction haulage and also for special purposes (such as fire engines). Nowadays Scania produces Euro 6 trucks with improved fuel efficiency and hybrid technology buses. In 2014 Scania delivered 73015 trucks (47% in Europe alone) and 6767 buses (20% in Europe alone). In 2014 Scania was the fourth largest truck brand in Europe, with 33% of the total European production.

The main products of Scania CV AB are medium and heavy-duty diesel engines for road vehicles, based on four-stroke water-cooled engines with a power range between 120 kW and 540 kW. When dealing with heavy-duty trucks and large vehicles like buses a very important parameter is the effect of the product on the environment and Scania is at the frontline to design products in order to reduce emissions. The combustion process is related to engine performance and emissions, both parameters dictate the entire engine design. Performances need to be optimized with regard to the engine purpose, and exhaust emissions need to be in between the international regulations given by the European Union (and based on the Kyoto's Protocol). In particular the emissions that need to be verified are: carbon monoxide CO (negligible for diesel engine), unburned hydrocarbon HC and nitrogen oxides NO_x. At present Scania produces engines fulfilling Euro 6 legislation, the latest exhaust standard defined by the European Union. While the toxic emissions are regulated by the European legislation, there is no regulation about the limit value concerning the CO_2 emission, however there are target values for each type of engine and vehicle. Even without regulation the optimization of fuel economy and CO_2 emissions is a primary goal for Scania.

A way to reduce emissions is to have a complete combustion inside the cylinders although Diesel engines have a typical problem: it is difficult to obtain complete combustion of the fuel because of a usually slow fuel-air mixing rate. The main method to

have the most homogeneous combustion possible is to optimize the design of the cylinder and the cylinder head to have the desired flame front and propagation. The main parts that need to be designed in detail are:

- cylinder head;
- piston shape;
- inlet port geometries;
- fuel-injection device.

The flame front and then the combustion are influenced by the internal gas dynamics of the engine. In particular, the main parameters that drive the combustion are the macro flow modes inside the cylinder: Swirl and Tumble. Studies show that the major influence on the flame propagation is given by the Swirl mode, so the cylinder heads are designed to get the optimal Swirl Number in the cylinder. Unfortunately the Swirl Number is affected by many parameters, themselves influenced even by the production processes of the cylinder heads. Due to the large number of variables that affect the Swirl Number, random cylinder heads from the production chain are used as samples to be tested to verify the effective Swirl Number.

Another very important parameter is the Flow Coefficient, or $\mu\sigma$, the ratio between the actual air flow and the ideal one. Swirl Number and Flow Coefficient can be tested with the same apparatus. At present the test is performed in a test flow bench with an impulse swirl meter and the data are acquired in discrete time with 15 stationary valve positions of 1 mm lift (otherwise called steps), resulting in a test with a mean duration of 25 minutes. Considering the time to bring the cylinder head sample from the production sites all over the world to the central laboratory, the waiting list resulting from the long time needed to test every cylinder head and the test duration itself, in the event of a problem (Swirl Number outside the tolerance) the company will suffer a big economy loss, due to the recall a large amount of engines.

The main goal of this *project* is then to reduce the test duration to allow a shorter verification time, and if possible to create a simple set up for the test such that it will be possible to perform the test directly at the production site. To obtain the goal the idea is to investigate the possibility to perform the test in continuous time.

The results of the experimental procedures show that continuous operation is possible and that the flow inertia due to the valve motion has a small effect on the mean results (Swirl Number and Flow Coefficient). Considering the experimental tests performed the optimal set up for continuous tests seems to be: maximum Reynolds number of 55000, valve velocity 1.7 mm/sec, cycle motion, 10 cycle repetition. This configuration result in a test time of 10 minutes, hence the time saved respect to the stationary test is the 65%.

The chapters of this thesis will follow the project steps, to have a chronological and logical sequence of every phases.

Cylinder Gas Dynamics (2) presents a brief introduction to the main gas dynamics principles that govern the flow in the engine and in particular in the cylinder head, and more specifically Swirl Number and $\mu\sigma$ definition.

Swirl Number Evaluation (3) presents two experimental setups used at present to evaluate the Swirl Number and the calculation necesary to compute the mean Swirl Number.

Original Test Bench And Stationary Test (4) presents the stationary test bench, as the rig is used at present, and how the standard stationary test is performed.

Experimental Setup And Procedures (5) presents the first experimental phase of the project: the rig investigation. In this section the results of the tests performed are explained in order to clarify how the test bench works and its physical limit in order to establish the setup for the continuous tests.

Rig Calibration Procedure (6) presents the results of the calibration performed on the rig flow meter. The calibration was necessary in order to use the instrument without constant pressure drop over it.

Experimental Test With Continuous Acquisition (7) presents the results of the continuous tests, for both high and low Swirl Number reference cylinder heads. This section presents subsections for each type of test performed: the series of tests performed to decide the main rig setups to be investigated, the repeated tests performed with the previously chosen setups, the tests performed considering cycling motion as in real engine behaviour and the tests performed to define the minimum number of cycles needed to get an acceptable result.

Flow Inertia Effect (8) presents the flow inertia study to verify the assumption that the inertia does not effect the mean results of the test performed with continuous motion of the intake valves.

Axial Velocity Distribution in the Cylinder (9) presents the experimental study performed with Laser Doppler Anemometry to investigate the axial velocity distribution.

Energy Peak Investigation (10) presents the experimental investigation of the energy peak found in *Chapter 9*.

Conclusions is the section that summarizes all the results of this project and to establish if the main goal was achieved.

Recommendations for future work is the last section of this thesis and presents the suggestions for future works related to this project.

To apply for a request to obtain further information, please contact the author or Scania[1].

[1]Chiara Olivieri, chiaraolivieri92@gmail.com
Björn Lindgren, bjorn.lindgren@scania.com

Chapter 2

Cylinder Gas Dynamics

Cylinder gas dynamics describes how the air moves inside the cylinder, it is used also to describes how fuel is mixed with air and how the combustion flame propagates. Cylinder gas dynamics, as the combustion, is therefor governed by the intake process and cylinder head characteristics.

Fluid motion inside the cylinder starts with the intake process and continues with the fluid interaction with cylinder walls and piston. The intake process generates two large-scale turbulent rotating flow patterns called *Swirl* (the circulation of the air around the cylinder axis) and Tumble (the axial circulation of the air) (Figure 2.1), these patterns can be controlled by detailed design of the inlet channel and the valves' seat but they will eventually breakdown in $3D$ turbulent structures with smaller scale.

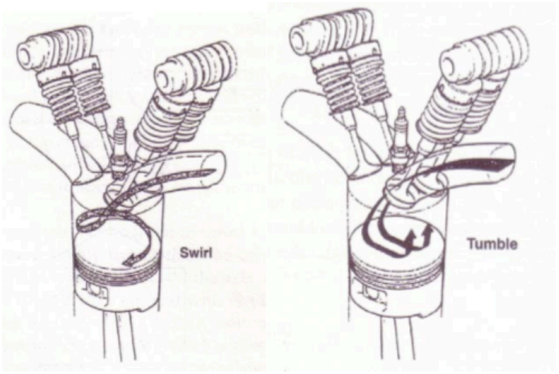

FIGURE 2.1: Schematic example of Swirl and Tumble. From [1]

The highly turbulent behaviour that allows the required air-fuel mixing is governed by the classic turbulence theory slightly modified to take into account the repetition of non-identical flow patters during different engine cycles, the so call *cycle-to-cycle variation*. The cycles repetition in a working engine gives flows that can be assumed as quasi-periodic, consequently an *ensemble-averaging* can be used that in the engine case is the mean value at a specific crank angle α in the basic cycle [2]. Defining the instantaneous velocity for each crank angle, α, and cycle, i, as

$$U(\alpha;i) = \overline{U}(\alpha;i) + u(\alpha;i) \tag{2.1}$$

where $\bar{U}(\alpha;i)$ and $u(\alpha;i)$ are the mean velocity and the fluctuating velocity at crank angle (α) and cycle (i). The ensemble-averaged velocity is

$$\overline{U}_{EA}(\alpha) = \frac{1}{N_c} \cdot \sum_{i=1}^{N_c} U(\alpha;i) \tag{2.2}$$

where N_c is the total number of cycles considered. Furthermore it is necessary to consider the differences between the ensemble-averaged velocity and the mean velocity per cycle:

$$\hat{U}(\alpha;i) = \overline{U}(\alpha;i) - \overline{U}_{EA}(\alpha) \tag{2.3}$$

Now it is possible to define the instantaneous velocity per crank angle and cycle as

$$U(\alpha;i) = \overline{U}_{EA}(\alpha) + \hat{U}(\alpha;i) + u(\alpha;i) \tag{2.4}$$

Turbulent flows, as the one in the engine cylinder are characterized by three lengths and times scales (Figure 2.2):

- Integral scales l_I and τ_I;
- Taylor scales (or microscale) l_M and τ_M;
- Kolmogorov scales l_K and τ_K.

The *Integral length scale* defines the dimension of the large turbulent structures (large eddies) while the *Integral time scale* defines the amount of time necessary for a large eddies to move to another position. Following the energy cascade, the breakdown of the large structures generate smaller structure characterized by the *Kolmogorov scales*, dissipative scales. In between the Integral macroscales and the dissipative Kolmogorov scales the turbulent structures can be characterized by microscales, *Taylor scales*.

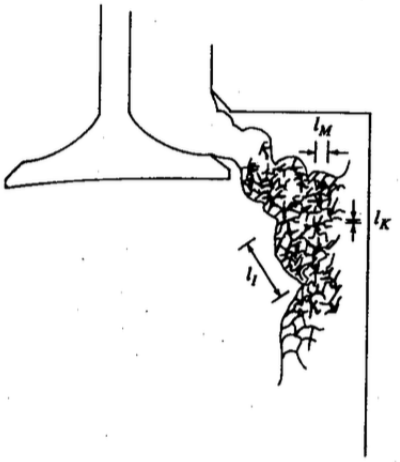

FIGURE 2.2: Characterstics turbulence lengths in engine cylinder. From [2]

2.1 Swirl

Swirl is the flow mode that causes the circulation of the air around the axis of the cylinder. The fluid in the cylinder will hence follow an organized helical path through the cylinder, from the cylinder head to the piston. Being an organized motion, which is less dissipative than free turbulence, Swirl is able to retain energy longer than other non organized flow modes, generating a high level of turbulence. As all the turbulent flows, Swirl mode will suffer a breakdown, however in modern combustion chambers Swirl is able to survives TDC (top dead centre) and never break into turbulence, resulting in a perfect way to control the flame propagation and the combustion [1]. Swirl is characterized by the *Swirl Number*: a ratio to compare the angular momentum with the axial momentum of the flow

$$N = \frac{\omega \cdot R}{V_z} \tag{2.5}$$

where ω is the angular velocity of the flow, R the cylinder radius (or another characteristic length) and V_z is the mean axial speed of the piston.

2.1.1 Swirl Generation

Swirl can be produced through:

- opening one inlet valve more than the other;
- with a particular geometry of the inlet ports;
- with a masked cylinder head.

2.1.2 Valves Opening To Generate Swirl

Opening the valves differently is a strategy that can be applied only in cylinder heads with two inlet valves. Theoretically to generate Swirl it is simply necessary to open the two inlet valves with different lift, however experimental tests show that to get significant Swirl Number it is necessary to keep one valve almost completely closed but for the fuel injection. Keeping one valve closed implies low air flow, thus a fuel-rich cloud, therefor this solution helps the creation of a stratified charge.

2.1.3 Inlet Port Geometry To Generate Swirl

The main ways to generate Swirl with inlet port geometry are two:

- injecting the air tangentially to the cylinder wall

- generating the Swirl motion directly within the inlet port itself.

Using inlet port with deflector wall or direct port tangentially to the cylinder wall (Figure 2.3 a and b) the impact with the wall will cause a sideways and downward deflection that initiates the Swirl motion. Specially shaped inlet ports, such as shallow ramp helical and steep ramp helical ports (Figure 2.3 c and d), are able to generate Swirl prior to the air entering in the cylinder. Because the Swirl is generated in the intake channel this configuration is less sensitive to the relative displacement of intake channel and cylinder (that is a critical step in the production chain).

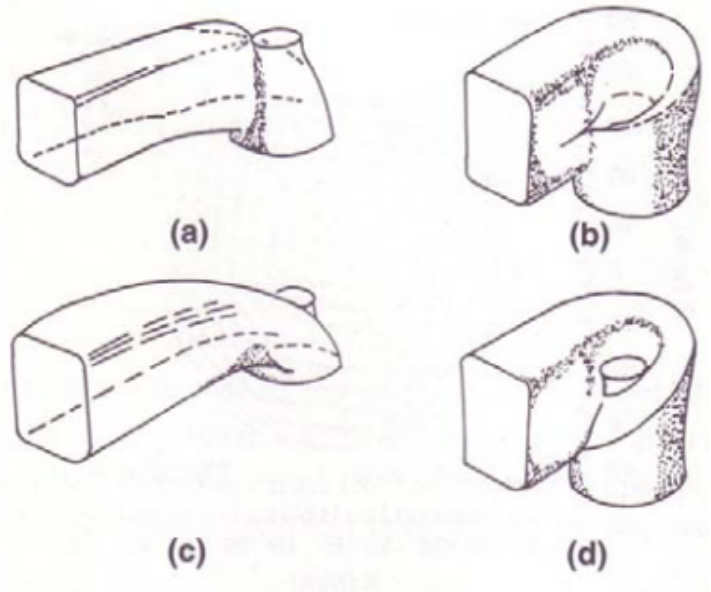

FIGURE 2.3: Different type of swirl-generating inlet port: (a) deflector wall; (b) directed; (c) shallow ramp helical; (d) steep ramp helical. From [2]

2.1.4 Masked Cylinder Head And Shrouded Inlet Valve

The configurations in Figure 2.4, for masked cylinder heads and shrouded valves, generate the same result as the direct or deflect wall inlet port. However both designs are rarely used in production engines because of the high cost but in respect to the previous case modification are easier to be made, therefor they are common in research engines.

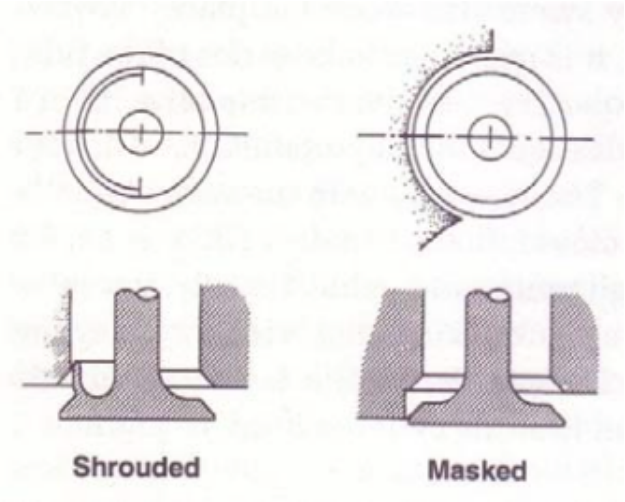

FIGURE 2.4: Shrouded inlet valve and masked cylinder head. From [2]

2.2 Flow Coefficient

The $\mu\sigma$ Coefficient, also called Flow coefficient, is a figure of merit that indicates the ratio of the actual air flow and the ideal one at a given pressure drop over the channel. Defining q_{eff} as the measured mass flow, and q_{theo} is the theoretical flow rate, then the $\mu\sigma$ coefficient will be

$$\mu\sigma = \frac{q_{\text{eff}}}{q_{\text{theo}}} = \frac{q_{\text{eff}}}{A_0 \cdot w_2 \cdot \rho} \tag{2.6}$$

where w_2 is the velocity after the inlet valves and the valve area is computed considering all the inlet valves present in the cylinder head:

$$A_0 = \frac{n \cdot (\pi \cdot d^2)}{4} \tag{2.7}$$

where n is the number of valves and d is the diameter of the valves.

Assuming no losses, incompressible flow, isentropic processes and constant density (ρ), Bernoulli's Equation holds (see Figure 2.5)

$$p_1 + \frac{\rho \cdot w_1^2}{2} = p_2 + \frac{\rho \cdot w_2^2}{2} \tag{2.8}$$

then given $w_1 = 0$ and $p_1 - p_2 = \Delta p$, the velocity after the inlet valve will be

$$w_2 = \sqrt{\frac{2 \cdot \Delta p}{\rho}} \tag{2.9}$$

To compute the Swirl Number it is necessary to know the environment characteristics, such as air pressure p [Pa], air density ρ [kg/m^3] and temperature T [K]. Given the assumption of incompressible flow the density ρ can be computed knowing pressure p and temperature T as

$$\rho = \frac{p}{R \cdot T} \tag{2.10}$$

where R is the ideal gas constant.

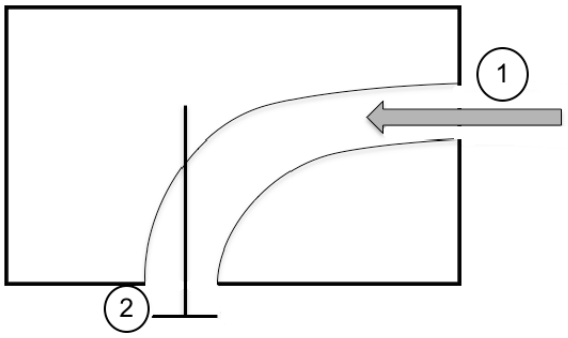

FIGURE 2.5: Schematic of intake channel. From [3]

Chapter 3

Swirl Number Evaluation

The Swirl Number, defined in *Chapter 2* as

$$N = \frac{\omega \cdot R}{V_z}$$

can be tested, in a test bench blowing air through the cylinder head, with two main experimental setups:

- Paddlewheel Test (Section 3.1)
- Honeycomb Test (Section 3.2)

In the following we will describe how these two methods can be compared and how a mean Swirl number over an opening cycle is computed.

3.1 Paddlewheel Test

The experimental setup for the paddlewheel test, Figure 3.1, consists of a paddlewheel positioned after the cylinder head in the mock-up cylinder. In this case the Swirl Number is calculated as the ratio between the paddlewheel speed (n_D) and the fictitious engine speed (n)

$$N = \frac{n_D}{n} \tag{3.1}$$

Considering the fictitious engine speed n that gives to the piston the average speed $c_m = w_2$ corresponding to the airflow q_{eft} it is possible to write

$$c_m = \frac{s \cdot n}{30} = \frac{q_{eff}}{A_{cyl} \cdot \rho} = w_2 \tag{3.2}$$

where $A_{cyl} = \pi D^2/4$ is the cylinder area. Consequently

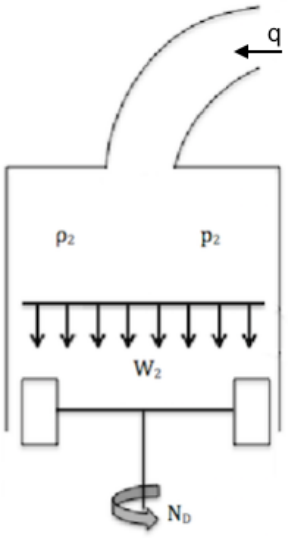

FIGURE 3.1: Paddlewheel test setup scheme.

$$q_{eff} = w_2 \cdot A_{cyl} \cdot \rho \tag{3.3}$$

then, solving the Equation 3.2 for n it gives

$$n = \frac{30 \cdot q_{eff}}{s \cdot A_{cyl} \cdot \rho} = \frac{30 \cdot q_{eff}}{V_z \cdot \rho} \tag{3.4}$$

and finally

$$\frac{n_D}{n} = \frac{n_D \cdot V_z \cdot \rho}{30 \cdot q_{eff}} \tag{3.5}$$

However the paddlewheel rotation depends on the radial position of the wheel and on their design, thus any result obtained with this setup should consider a correction parameter to take into account the above mentioned dependencies.

3.2 Honeycomb Test

The second, and at present more common, setup to test the Swirl is shown in Figure 3.2. In this case the angular velocity of the flow is not measured through a paddlewheel but with a honeycomb matrix positioned at the bottom of the mock-up cylinder. The advantage of this setup is that the honeycomb related data are not dependent on

the position nor on the geometry of the honeycomb matrix because the matrix lay on the total area of the cylinder without interference with the flow.

The principle of this setup is that the honeycomb elements will be subjected to a torque (M) caused by the angular momentum given by the Swirl mode. Assuming that the velocity in the radial direction has a linear distribution, the measured torque (M) can be related to the angular velocity (ω) as show in the following.

By definition the torque (M) is equal to the angular momentum flux $\dot{I}$

$$M = \dot{I} = \int_A d\dot{I} \tag{3.6}$$

then expressing $d\dot{I}$ as function of $d\dot{m}$

$$d\dot{I} = (\omega \cdot r) \cdot r \cdot d\dot{m} \tag{3.7}$$

$d\dot{m}$ as function of dA

$$d\dot{m} = dA \cdot V_z \cdot \rho \tag{3.8}$$

and dA as function of $d\varphi$

$$dA = dr \cdot r \cdot d\varphi \tag{3.9}$$

it is possible to conclude that

$$d\dot{I} = \omega \cdot r^3 \cdot dr \cdot d\varphi \cdot V_z \cdot \rho \tag{3.10}$$

so

$$M = \dot{I} = \int_A d\dot{I} = \int_0^R \int_0^{2\pi} \omega \cdot r^3 \cdot dr \cdot d\varphi \cdot V_z \cdot \rho \tag{3.11}$$

Furthermore, considering that the axial velocity can be written as

$$V_z = \frac{q_{eff}}{\rho \cdot A_{cyl}} \tag{3.12}$$

it is possible to write

$$M = \frac{\omega \cdot q \cdot D^2}{8} \tag{3.13}$$

Finally the angular velocity can be expressed as

$$\omega = \frac{8 \cdot M}{q \cdot D^2} \tag{3.14}$$

Knowing the angular velocity (ω) is it possible to compute the Swirl Number using two different ratios:

- Spin Ratio (Section 3.2.1)
- Speed Ratio (Section 3.2.2)

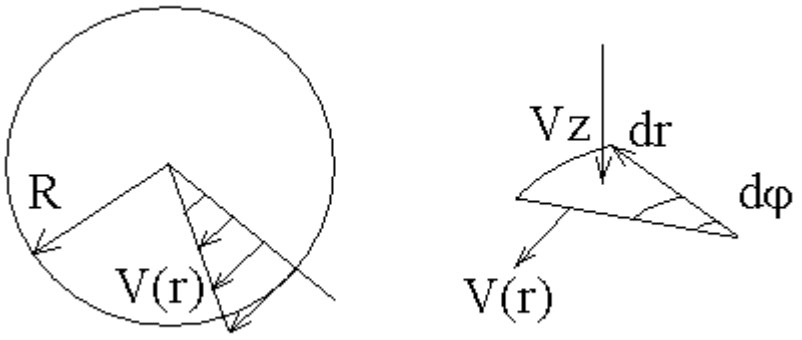

FIGURE 3.2: Honeycomb test setup scheme. From [3]

3.2.1 Spin Ratio For Honeycomb Setup

The spin ratio is a Swirl evaluation method to obtain the same comparison relation of the paddlewheel test case: the ratio between paddlewheel velocity (n_D) and engine speed (n), $N = n_D/n$, both given in [rpm].

The paddlewheel velocity is a fictitious velocity computed with the angular velocity (ω) and the torque (M), as (see Equation 3.14)

$$n_D = \frac{60 \cdot \omega}{2 \cdot \pi} = \frac{M \cdot 60}{q_{eff} \cdot A_{cyl}} \tag{3.15}$$

Considering the same engine velocity (n) of the paddlewheel setup in Equation 3.4 the Spin Ratio can be express as

$$\frac{n_D}{n} = 2 \cdot s \cdot \frac{M \cdot \rho}{q_{eff}^2} \tag{3.16}$$

The Swirl Number computation in Equation 3.16 is the one used in the Scania test bench and used in this *Thesis*.

3.2.2 Speed Ratio for Honeycomb Setup

The Swirl Number can also be calculated as the ratio between the tangential velocity ($V(r)$) and the axial velocity (V_z), Figure 3.2,

$$N = \frac{V(R)}{V_z} \tag{3.17}$$

considering V_z as in Equation 3.12 and $V(R)$ as

$$V(R) = \omega \cdot R \tag{3.18}$$

The Swirl Number can hence be written as

$$N = \frac{V(R)}{V_z} = \frac{\omega \cdot R}{V_z} = \frac{8 \cdot M}{q_{eff} \cdot D^2} \cdot \frac{D}{2} \cdot \frac{\rho \cdot A_{cyl}}{q_{eff}} = \pi \cdot D \cdot \frac{M \cdot \rho}{q_{eff}^2} \tag{3.19}$$

3.3 Mean Swirl Number calculation

The Swirl Number defined in Equation 3.1 as the ratio between the paddlewheel velocity and the engine velocity $n = 30 \cdot c_m/s$, can also be expressed as

$$\frac{n_D}{n} = \frac{1}{V_s} \cdot \int_0^{V_s} \frac{n_D}{n}(V) \cdot dV \tag{3.20}$$

where the volume stroke (V_s) is related to the mass flow (q_{eff}) as following

$$\frac{q_{eff}}{\rho} = \frac{2\pi}{60} V_s \tag{3.21}$$

However while performing a simulated intake stroke in the Swirl evaluation test, the instantaneous velocities and the velocity function of the crank angle are related

$$\frac{n_D(\alpha)}{n} = N(\alpha) \cdot c(\alpha) \cdot \frac{30}{s \cdot n} \tag{3.22}$$

The ratio between the instantaneous and mean piston velocity can be written in terms of the change in piston position as

$$\frac{c(\alpha)}{c_m} = \pi \cdot \frac{dz(\alpha)}{d\alpha} \tag{3.23}$$

giving

$$\frac{n_D(\alpha)}{n} = N(\alpha) \cdot \pi \cdot \frac{dz(\alpha)}{d\alpha} \tag{3.24}$$

The change in volume can be written

$$dV = V_s \frac{dz}{d\alpha} d\alpha$$

and using the instantaneous Swirl Number as in Equation 3.20, it is possible to write

$$\left(\frac{n_D}{n}\right)_{medium} = \frac{1}{V_s} \cdot \int_0^{V_z} N(\alpha) \cdot \pi \cdot \frac{dz(\alpha)}{d\alpha} \cdot V_s \cdot \frac{dz}{d\alpha} \cdot d\alpha \tag{3.25}$$

and to conclude

$$\left(\frac{n_D}{n}\right)_m = \pi \cdot \int_0^{\pi} N(\alpha) \cdot \left(\frac{dz(\alpha)}{d\alpha}\right)^2 \cdot d\alpha \tag{3.26}$$

In the a similar manner (although the details are not given here) the average value of the flow coefficient ($\mu\sigma$) can be calculated.

Chapter 4

Original Test Bench And Stationary Test

The test bench in use to perform Swirl Number and $\mu\sigma$ computations in stationary conditions, in Figure 4.1 and schematically in Figure 4.2 is equipped with:

- The tested cylinder head (1);
- The valve lifter (2);
- A mock-up cylinder (3);
- An impulse swirl meter (ML);
- Two settling chamber (after the cylinder head, 5, and before the driving fan, 8);
- A rotary piston flow meter (6, NL);
- Electrical motors to drive the flow meter (7) and the fan (11);
- A five-way bypass valve (9) to control the pressure drop below the cylinder (hence the flow direction and Reynolds number);

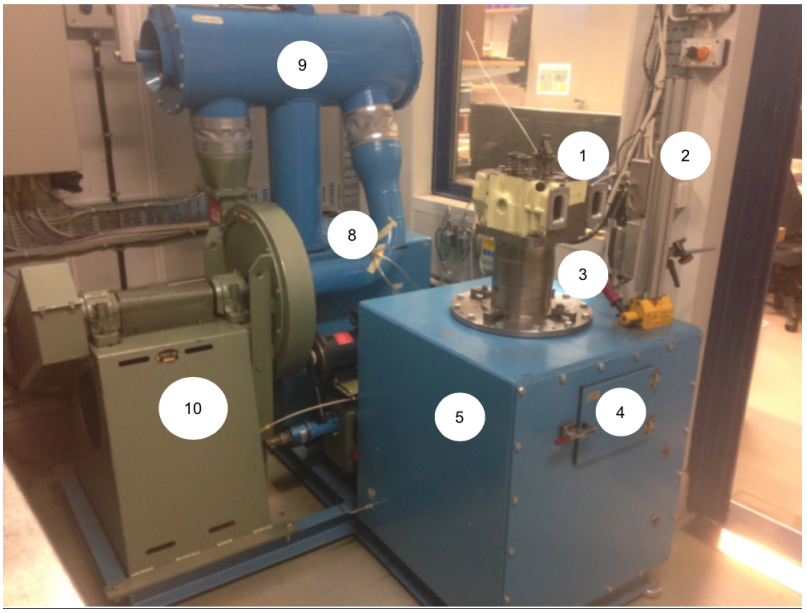

FIGURE 4.1: Original rig

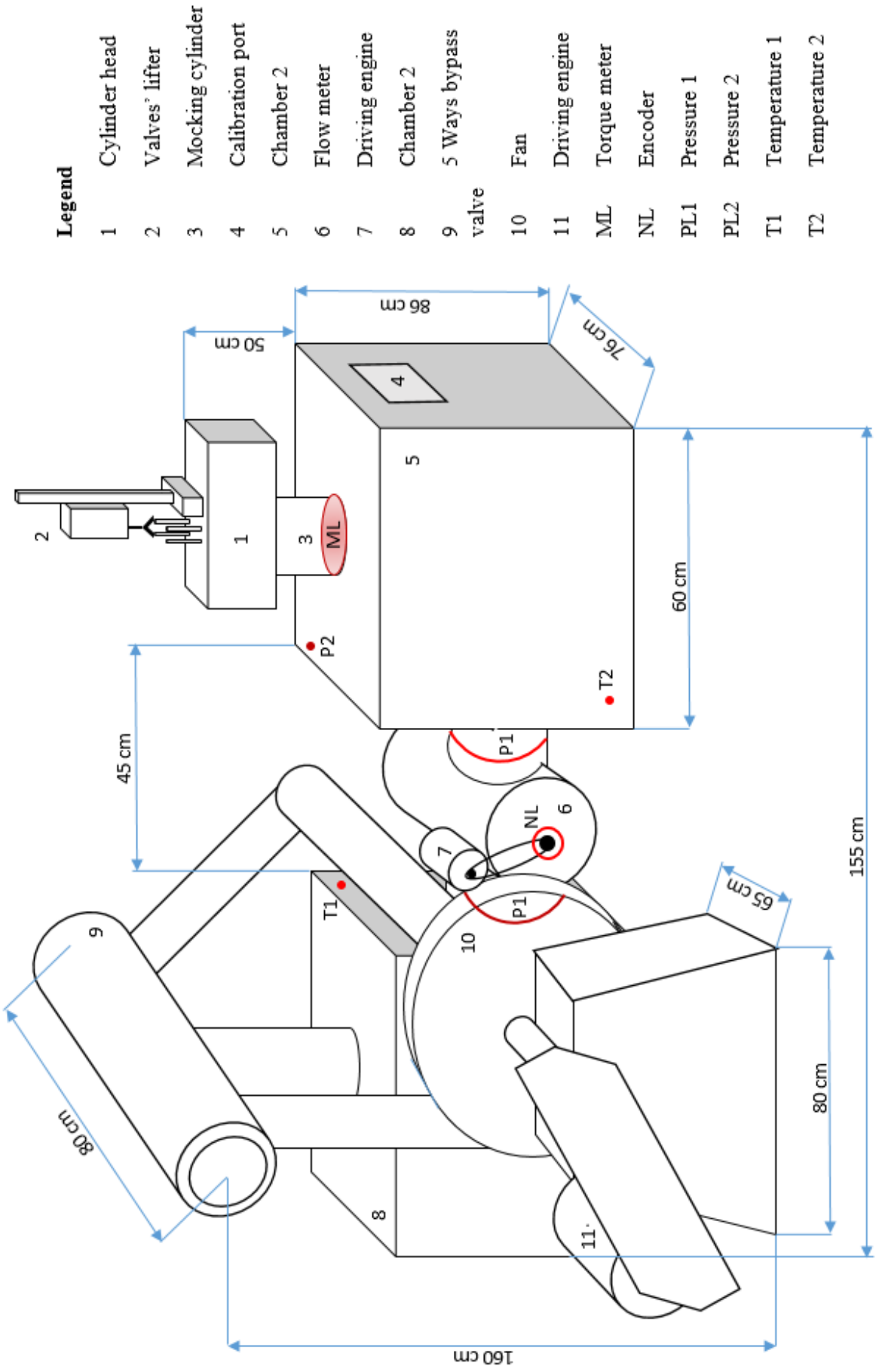

FIGURE 4.2: Test bench scheme

- A motor to drive the bypass valve (not shown);

- A fan to drive the air in the bench (10);

Furthermore in the rig are used:

- pressure sensors (PL1, PL2);

- temperature sensors (T1, T2);

- torque meter (ML);

- distance sensor (2);

- *rpm* sensor (NL);

- voltmeter (not shown).

4.1 Impusle Swirl Meter

The impulse Swirl meter, *Cussons P7300*, measure the Swirl with a honeycomb matrix linked to a load cell that restrain the matrix rotation. The honeycomb matrix in Figure 4.3, is mounted on a shaft and it is supported by precision ball bearing and it is suspended in an annular oil reservoir that act both as air seal and as viscous damper (to reduce the signal fluctuations).

The Swirl meter measure the angular impulse given by the angular velocity component as a torque, for this reason the Swirl meter is also called torque meter. The angular velocity is caused by the interaction between the rotating flow with the cells in the honeycomb matrix, that consequently is force to rotate. The torque measurement is allowed by a torque arm connected to the axle of the honeycomb matrix and acting on a Wheatstone bridge strain-gauge transducer.

The Swirl meter drifts and it needs to be calibrated at least twice a day. The calibration process is made by few steps:

- Set the Zero of the impulse torque meter to 0;

- Add to the Swirl meter, on the special shaft and wheel, the calibration mass (1000 g);

- Set the Span to ± 1000;

- Remove the weight and close the door;

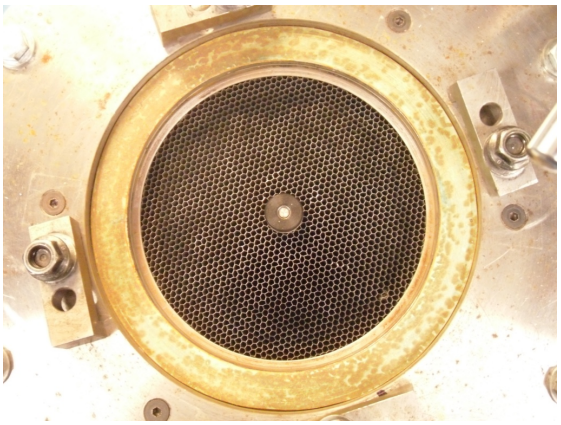

FIGURE 4.3: Torque meter - Honeycomb matrix

- Check the Zero of the impulse meter (in case different from zero repeat the calibration procedure).

4.2 Flow Meter

The flow rate is measured by an *Aerzen* rotary piston gas meter *G40* with lobed impeller. Because it works by volume displacement, to following the given calibration map, it is necessary to have the pressure drop at the impeller equal to zero. Then the velocity of the motor that drive the flow meter is proportional to the mass flow through the test bench. The speed [rpm] of the electric motor is also used as check parameter for eventual leak in the system: with closed valves the speed of the motor should be zero.

The flow meter is one of the main instrument to take in account in this work. In particular it will be necessary to understand if the instrument will be able to work without the stabilization phase, thus with non-zero pressure drop over itself.

4.3 Five-Way Bypass Valve

The five-way bypass valve, driven by an electrical motor, is used to control the pressure in the chamber under the cylinder. In other words the bypass valve is the instrument with which is possible to control the flow direction and the Reynolds number.

4.4 Fan

The fan used to drive the air into the test bench is a centrifugal fan belt drive *HMB10H2* by *äkt Miljösystem*, with curved blades. The driving motor is an *ABB MBT1328A*. The fan is operated at a constant speed at maximum power to provide the correct air flow during the test.

4.5 Stationary Test Protocol

The stationary test conducted at Scania laboratory can regard both intake stroke and exhaust stroke. The differences are that in the former case only the intake valves are moved and the air is sucked from the rig through the test bench, while in the latter only the exhaust valves are moved and the flow direction is opposite to the former case.

The test is usually performed with 1 mm lift between measurement points (valve lift), however the step size can be modified by the operator changing the computer code. Considering steps in between 15 mm and 1 mm lift, the test takes around 25 minutes to be completed. Once that the operator has mounted the cylinder and the cylinder head on the test bench, he can launch the computer software for the test. The *LabVIEW* program automatically sets every instrument in the rig to the chosen starting value (Table 4.1) and sets the tolerance for every parameter.

TABLE 4.1: Starting value for the main parameters during the stationary test

Parameter	**Variable**	**Intake Test**
Valves Lift	$AT02$	15 mm
Bypass Position	$AT01$	2.50 V
Δp over the cylinder		
Leakage control	$PL02$	-2500 Pa
Test value	$PL02$	-2450 Pa

Once that every parameter is at the correct value the program starts the *Leakage Test* to verify that no leakage is present in the test bench. Leakages can happen in every part of the rig and can be caused by ageing damages but also by unusual damages or incorrect cylinder head positioning. The Leakage Test is performed with closed valves and by setting the bypass position to obtain the requested pressure drop over the cylinder (in case of intake test $PL02 = -2500$ Pa). When the pressure drop is gained the program verifies that the flow meter rotations are less then the limit value chosen by the operator (at present 50 rpm). If the Leakage Test fails the test is aborted and a warning message is displayed, otherwise, if the Leakage Test is successfully passed, the bypass valve moves to gain the predefined test value of the pressure drop over the cylinder.

As soon as the pressure drop over the cylinder is at the right value for the test the program *Sets the Valves Position* at the starting value (15 mm for the intake test).

When the valves are at desired position the *Stabilization Phase* begins: the pressure drop over the flow meter and over the cylinder need to be stable at the chosen values (respectively 0 Pa and -2450 Pa).

Because the pressure drops are dependent on each other the Stabilization Phase is made in three steps:

- pressure drop over the cylinder set to the desired value by moving the bypass valve;
- pressure drop over the flow meter set to zero by regulating the rotation of the driving engine;
- re-regulation of the pressure drops until the desired values are obtained.

The Stabilization Phase is performed in a limited amount of time, if this time ends before stable pressure drops are gained the process is interrupted, the tolerances of each parameter are enlarged and the Stabilization Phase begins again with the new tolerances. As every previous steps of the test, the Stabilization needs to happen before the *Time Out*, a time value fixed to limit the duration of the test and its accuracy (the time out limits the number of tries and hence the increasing of the tolerances).

Once the flow is stabilized the *Measure* can begin. At present the program measures: environment parameters, torque and flow-meter rotations. If during the Measure some parameter goes outside of its limits the Measure is aborted and the process begins again from the Stabilization Phase. If the Measure is correctly performed the program moves the valves to the next position, according to the *Step Size* chosen, and the process starts again from Stabilization Phase.

When the last measure (the final valve position) is concluded the program automatically computes the flow rate for every step measured during the test and it *Saves the Results* to the designated file. The *Output File* is evaluated by a *Matlab* program that computes:

- Mean Swirl Number;
- Mean $\mu\sigma$ Coefficient;
- Swirl Number for each lift position;
- $\mu\sigma$ for each lift position;

- Torque for each lift position;

- Mass flow rate for each lift position;

4.6 Cylinder head

Two cylinder heads were studied. The high Swirl Number reference cylinder head is a cylinder head designed for extremely high inlet pressure and that fulfils Euro 5 legislation, whereas the low Swirl Number cylinder head fulfil the Euro 6 legislation. The cylinder and cylinder head parameters are shown in Table 4.2.

TABLE 4.2: Cylinder and cylinder head parameters

Parameter	**Unit of Measure**	**Measure**
Stroke	mm	160
Connecting Rod	mm	255
Cylinder Diameter	mm	130
Intake valve seat diameter	mm	39.7
Intake valve seat angle	deg	20
Inlet area	mm	1385
High swirl cylinder head	$(n_D/n)_m$	2.1
Low swirl cylinder head	$(n_D/n)_m$	1.3

Chapter 5

Experimental Setup And Procedures

This chapter describes the dynamical behaviour of the rig. Experimental tests were operated in order to understand the limits of the instruments that together form the rig and if continuous tests were possible.

5.1 Valve Lifter Velocity Investigation

The valve lifter has constant velocity in the central region of the motion, but not in the starting phase nor in the final phase. In the starting phase its speed increases to reach the constant value and at the final phase it slows down to allow the valves to reach the exact position. However, from the results of the tests it is possible to get the total amount of time needed to cover the entire range of motion, i.e. 15 mm. The speed computed from the data acquired is an average speed that does not take in account neither the acceleration phase nor the deceleration phase. This is however of marginal interest with respect to the total amount of time needed to complete the valve movement.

The results of the investigation are reported in Table 5.1, and from now on the valve lifter velocity will be indicated with the value of the control parameter.

TABLE 5.1: Average speed and total amount of time to cover 15 mm for eight control parameter values

Control Parameter (BT02VEL)	**Average Speed** [mm/s]	**Total Time** [s]
1	0.01	—
100	0.30	55
150	0.40	40
200	0.50	30
250	0.55	28
300	0.60	25
350	0.65	23
400	0.70	20

5.2 Bypass Position Investigation

The investigation regarding the position of the bypass valve shows that positions larger than 2.4 (value of the control parameter) will result in a positive pressure difference between the chamber under the tested cylinder head and the ambient, thus in a reverse flow through the test bench. The reverse flow cannot be seen in the flow meter velocity data because the encoder is only able to acquire the number of rotations but not the direction.

On the other hand, bypass valve positions smaller than 0.8 will result in too small Reynolds number to get correct result from the post-processing evaluation. Also, with bypass valve around 1.4 the pressure drop over the cylinder is approximately the one previously used for PIV measurements. Therefore, the most interesting bypass valve positions range is the one in between 0.8 and 1.4.

5.3 Intake Valve Lifter Velocity and Bypass Valve Position Investigation

An investigation of the combined effect of different valve lifter velocity and bypass position was performed to understand the relation of these two parameters. Every valve velocity shows a similar type of behaviour when opening the bypass valve (increasing its position):

- The pressure drop over the cylinder increase;
- The flow meter velocity decrease;
- The honeycomb torque increase.

However there is a difference between the intake valve motion from 0 to 15 mm and the one from 15 to 0mm. Comparing the same intake valves motion it is visible a similar behaviour for every parameter studied:

- The pressure drop over the cylinder shows, for both the motions of the intake valves, slightly different behaviour when considering different intake valve velocities, indeed the curves do not overlap (as the torque ones). These differences can influence the computation of the final results, therefor will affect the choice of the future setup for continuous tests;
- The pressure drop over the flow meter shows, as the pressure drop over the cylinder, slightly different behaviour with different intake valve velocities;

- The flow meter velocity behaviour related to intake valves motion from 15 to 0 mm shows differences when considering different intake valve velocities only between 2 and 12 mm, around 0 and 15 mm lift the curves overlap;

- The flow meter velocity behaviour related to the intake valve motion from 0-15 mm shows that there is quite a big difference when considering different intake valve velocity around 0 mm lift that slowly decrease until the overlap around 15 mm lift;

- The torque behaviour is similar for each intake valves velocity, all the curves overlap. It is possible to identify three main region characterized by different slopes of the torque curve: 0-4 mm, 4-13 mm and 13-15 mm.

Investigating a cyclic motion of the valves, 0-15-0 mm, it is possible to notice that:

- The pressure drop over the cylinder has different behaviour during the different phases of the cycle and it seems scaled with the bypass valve position;

- The flow meter velocity shows hysteresis, the higher the valve velocity the larger the hysteresis;

- The torque, as the flow meter rotations, show hysteresis, the higher the valve velocity the larger the hysteresis.

5.4 Acquisition Frequency Investigation

All the instruments installed in the rig are able to acquire at 10 Hz except for the flow meter that can acquire up to only 1 Hz. Then a *LabView* code was created to be able to increase the flow meter acquisition frequency.

After the modification the flow meter velocity was acquired. The data acquired at 10 Hz were expected to overlap the ones acquired at 1 Hz in some point of every step, instead there was a gap in between. The gap seems depending on the presence of the engine's belt, the bypass valve position, the intake valve velocity and on the range of motion:

- The constriction imposed by the engine's brake seems to reduce the gap;

- Opening the bypass valve seems to reduce the gap in the 15-0 mm range of motion of the intake valve but to increase the gap in the 0-15 mm range;

- The gap seems to be reduced by lower speed of the intake valve.

Considering the accuracy, given by the modification of the computer code, it seems that the data acquired with the lower valve lifter velocity are closer to the 1 Hz data than the one acquired with higher valve lifter velocity. However the gap between 1 Hz and 10 Hz data in the range of motion 0-15 mm is always important. To overcome the problem given by the code modification, and to be sure to not make any error during further tests a new counter was added to the test bench instrumentation. With the new counter the flow meter is able to acquire at 10 Hz as all other instruments.

As expected the data show that the old counter ($NL00$) is less accurate and with lower time response respect the new counter ($NL00\ NEW$). Due to the big difference between $NL00$ and $NL00NEW$ for every intake valve position was computed the mean of the flow meter rotations indicated by the new counter and then the result was compared with the data from the old counter to assure the continuity in the results: no differences between the mean values of $NL00$ and $NL00NEW$ were founded. Consequently the results from continuous tests can be compared with the standard one (obtained with the old counter) and, if needed, the stationary test can be performed also with the new counter.

5.5 Summary

The test bench seems to be physically capable to be operated in continuous time:

- The range of valve lifter velocities chosen for the next phase of the project was: 200-400, that means 2-1.4 sec/mm;
- Valve lifter velocities less than 200 correspond to test time higher than 30 seconds, hence for the future tests will not taken in account;
- The bypass positions range chosen for future tests was: 0.8 - 1.4, to be able to reach Reynolds number in the region of the stationary test (maximum Reynolds number 60000) but also to have negative pressure difference between the cylinder and the ambient;
- The belt connecting the driving engine and the flow meter affect the response of the latter but the effect seems to be positive for the final result (a constriction of the flow meter response smooth the fluctuation of the signal). Considering that having the belt always in position easier to switch between stationary and continuous setup, the belt was kept in position for the rest of the study;

- All the following tests will be performed with the new additional counter to be able to acquire all the data at 10 Hz.

Chapter 6

Rig Calibration Procedure

In order to perform tests with continuous valve motion it is necessary to eliminate from the experimental process the stabilization phase. This particular phase of the test allows the flow to be stable around special conditions:

- constant pressure drop over the cylinder;

- zero pressure difference over the flow meter.

At present the flow meter is calibrated to operate only with null pressure difference over itself and does not exist a calibration map that take in account for non null pressure difference. Thus, to evaluate the data acquired in continuous tests, it is necessary to create a calibration map to relate pressure difference, flow meter rotation and flow rate.

6.1 Calibration Setup

To recalibrate the flow meter it is necessary to add to the rig instrumentation another flow meter that does not require calibration or already calibrated. With the additional flow meter it is possible to acquire all the usual data, and in particular the pressure difference over the flow meter and its rotations, and the flow rate through the test bench.

6.1.1 Additional Flow Meter

The additional flow meter chosen was an orifice plate flow meter, which is a differential pressure flow meter. This type of flow meter was chosen because:

- it has a good precision;

- it is easy to install and to modify.

The orifice plate flow meter does not need calibration, if installed according to the standard SS EN ISO 5167-2[4]. A thin plate with a hole in the center is inserted in the pipe, and with two circular series of pressure taps (one upstream the plate and one downstream) the pressure drop across it is measured. Assuming incompressible flow, the induced pressure difference can be related to the flow velocity using the Bernoulli

equation. Considering a correction coefficient, needed to relate the orifice diameter with the vena contracta, the mass flow can be easily computed.

The flow meter used in this *project* has an inner pipe diameter of 75 mm and an orifice diameter of 55 mm, hence a β of 0.74. The downstream section was measured 740 mm and the upstream section measured 760 mm.

6.1.2 Mass Flow Computation

Verified that all the requirements given by the standard were fulfilled, the mass flow rate can be computed with Equation 6.1 and consequently the volume flow rate with Equation 6.2.

$$q_m = \frac{C}{\sqrt{1-\beta^4}} \cdot \epsilon \cdot \frac{\pi}{4} \cdot d^2 \cdot \sqrt{2 \cdot \Delta p \cdot \rho_1} \tag{6.1}$$

$$q_v = \frac{q_m}{\rho} \tag{6.2}$$

where C and ϵ are the discharge coefficient and the expansion factor, respectively[4]. These values depend on the Reynolds number and in the present case are 0.6176 and 0.9929, respectively.

6.1.3 Installation

The additional flow meter, as show in Figure 6.1a, was installed over the settling chamber in the position usually occupied by the mock-up cylinder. To be installed in the cylinder location (135 mm), the flow meter that has smaller diameter was equipped with a connecting section. The orifice plate flow meter was built in two sections to allow the operator to change the orifice plate if needed.

The additional flow meter has six, equally separated, pressure tabs upstream and downstream the flange (distant from the flange respectively D and $D/2$), these are connected to a differential pressure transducer to acquire the differential pressure between ambient and flange and the one over the flange itself (Figure 6.1b).

The acquisition of the two differential pressures was performed manually by the operator, because it was not possible to connect the additional pressure transducer to

the computer due to too few inputs, therefor during the post processing analysis it is necessary to remember that the manual acquisition will affect the data with some error.

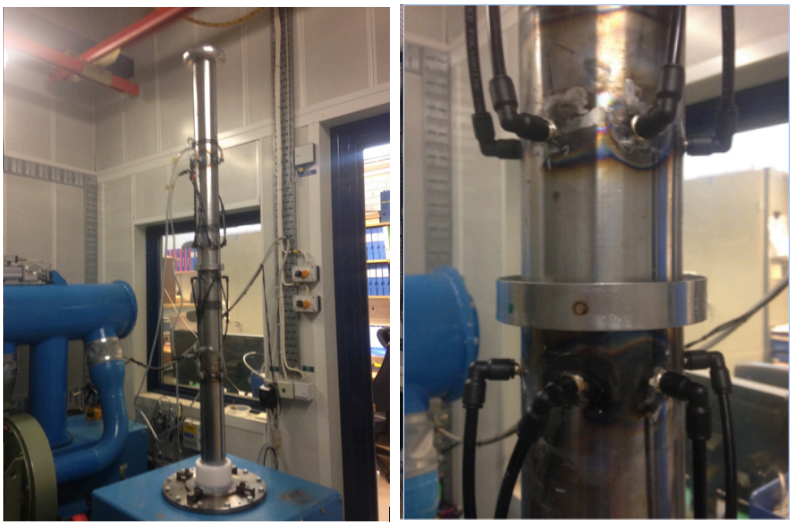

(a) Installation (b) Pressure taps

FIGURE 6.1: Orifice plate flow meters

6.2 Calibration Tests

The calibration tests were operated in such a way to reach flow rates normally reached during a stationary test and flow rates slightly higher. Therefor, considering the dimension of the additional flow meter, the tests were performed using bypass positions: 0.5, 0.8 and 1.1.

6.3 Calibration Map Computation

The data resulting from the calibration tests were processed manually, with a polynomial interpolation in $2D$, to obtain a surface and to force the calibration map through the origin (Figure 6.3). The coefficients of the surface that define the calibration map are:

$$[6.75 \times 10^{-5}, -2.32 \times 10^{-6}, 0].$$

The difference between the standard points and the calibration map, visible in Figure 6.2, is small and probably related to the human error occurred in the manual data acquisition.

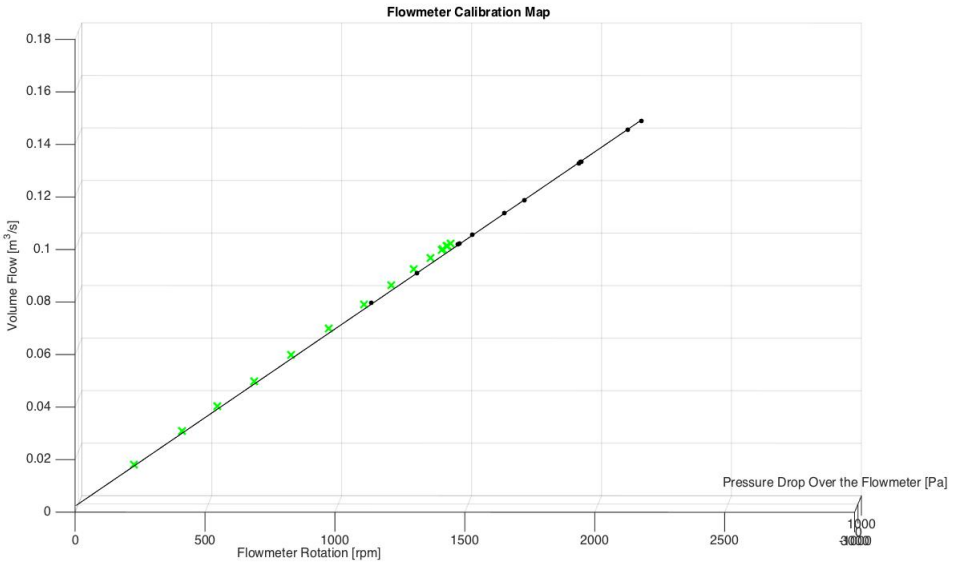

FIGURE 6.2: Final manual calibration map - Lateral view
Where: the solid line represent the calibration map, the black dots represent the calibration points and the green dots represent the points resulting from stationary test.

6.4 Summary

The calibration performed is considered acceptable for the purpose of this project: to understand if continuous measurements are possible for Swirl Number evaluation tests. Considering the calibration map obtained it will be possible to relate flow meter rotations to flow rate even in case of non-null pressure difference over the flow meter itself.

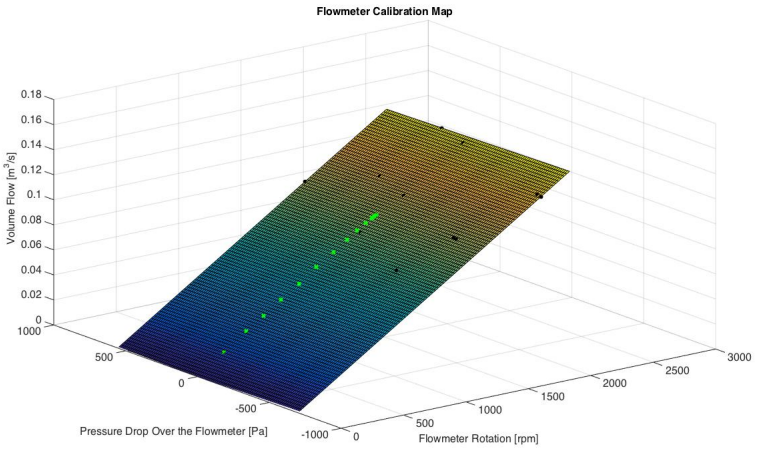

FIGURE 6.3: Final calibration map

Chapter 7

Experimental Test With Continuous Acquisition

This *Chapter* collects the main results from the continuous tests performed during the project. All the types of tests were conducted to understand if continuous valves motion was suitable for Swirl evaluation tests were performed with high (2.1) and low (1.3) Swirl Number reference cylinder head. This strategy was chosen to assume without loss of generality that the results obtained were independent on the type of cylinder head chosen for the study. The characteristics of both cylinder heads can be found in Table 4.2.

7.1 Experimental Setup And Procedures

The continuous tests were performed in four successive steps so that the latter step was depending on the result of the former one. The steps were the same for both high Swirl Number reference cylinder head and for low Swirl Number reference cylinder head:

- *Setup Definition Tests*: to define the optimal configurations setup for the cylinder head studied. In this first step the tests were performed in the two range of motions (opening and closing the valves), considering valves' lifter velocities from 200 to 400 at steps of 50 and were repeated for four bypass valve positions $(0.5, 0.8, 1.1, 1.4)$. All the tests were then evaluated to compare:
  - Range of motion;
  - Bypass valve position;
  - Valve lifter velocities.
- *Repeatability Tests*: to verify if the continuous tests were repeatable or if there is the need to perform repeated tests. The tests, performed in both range of motions with three valve lifter velocities (200, 300 and 400) were repeated ten times for each bypass valve position, 0.8 and 1.1.

- 5 *Cycles Tests*: to investigate the mean results considering few cycles of motion instead of separate range of motions. The cycles allow to acquire data during all test time, while using only a range of motion, and doing repeated tests, only half of the test time will produce useful data while the other half will be wasted. The tests were performed for bypass valve position 0.8 and 1.1 using only one valve lifter velocity, 300.

- *40 Cycles Tests*: to verify the number of cycles needed to gain stable mean results. The test were performed with the setup of the previous one, simply acquiring for around forty cycles instead of five.

7.2 Stationary Test Update

Because the standard test was usually performed considering only the opening range of motion and 15 points (with steps of 1 mm in between valve lifts) with the only purpose to compromise between duration time and results accuracy, a standard test with steps of 0.2 mm was performed in both range of motion to have a better visualization of the eventual differences in behaviour between the standard test and the continuous ones.

Using more experimental points, and considering also lift position in between 0 and 1 mm, it is possible to get results that are able to take in account for flow behaviour that otherwise are neglected (Figure 7.1). Moreover more steps allow to have more accurate mean results.

From now on the standard reference will be replaced with the one given by the standard test operated with more points, and eventually considering separately the two range of motions.

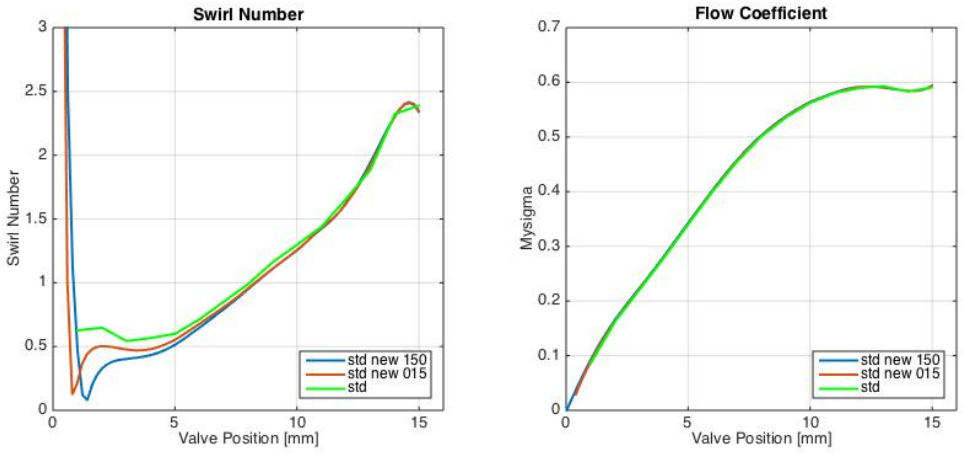

(a) High Swirl Number reference cylinder head

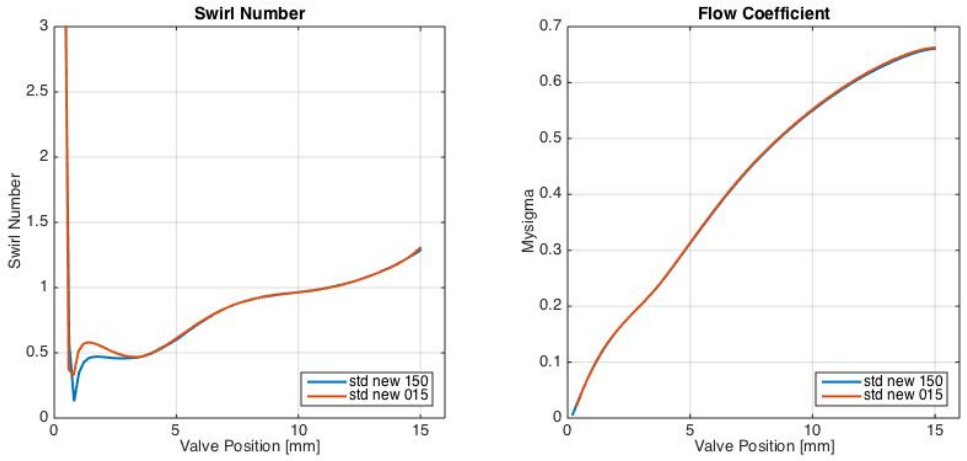

(b) Low Swirl Number reference cylinder head

FIGURE 7.1: Main parameters resulting from stationary test
Where in green are reported the results from the standard test with 15 steps between 15 mm and 1 mm lift closing the valve, in blue are reported the result from the stationary test performed with 80 steps between 15 mm and 0 mm lift closing the valve and in red are reported the result from the stationary test performed with 80 steps between 15 mm and 0 mm lift opening the valve

7.3 Setup Definition Tests

From the investigation tests it is possible to notice that the bypass position that gives pressure drop over the chamber below the cylinder similar to the one used during the standard test is bypass position 0.8. Bypass positions 1.1 and 1.4 give smaller pressure drops, similar to the ones used for PIV (Particle Image Velocimetry) or LDV (Laser Doppler Velocimetry) experiment. The same can be said for mass flow rate and Reynolds number, hence the *Setup Definition Tests* is performed with bypass position in between 0.5 and 1.4.

Looking at the graphs for instantaneous Swirl Number and $\mu\sigma$ Coefficient, Figures 7.2 and 7.3, it is possible to notice that the Flow Coefficient does not have important differences from the stationary result, however there are differences between the Swirl Number resulting from continuous test and the stationary one. In particular the differences seems to be larger between 0 and 5 mm lift. The bypass positions with behaviour closer to the stationary result are 0.8 and 1.1.

Figures 7.4 and 7.5 show the medium Swirl Number per bypass position (along the x axis) and per range of motion (opening motion in blue and closing motion in black). To have an immediate visualization in the same graph were reported the total mean value (in red) and the partial mean value per range of motion (opening motion in magenta and closing motion in blue). In case of high Swirl Number, it seems that the medium Swirl Number is clearly grouped per range of motion both with the same trend: medium Swirl Number decrease while increasing the bypass position. Opposite to the case of high Swirl Number, the low Swirl Number cylinder head does not show any trend in the medium Swirl Number. From these graph the worst bypass position seems to be 0.5.

Tables 7.1, 7.2 and 7.3 and 7.4 show the relative standard deviation from the stationary result of Swirl Number and Flow Coefficient for high Swirl and low Swirl, respectively. Swirl Number results have lower relative standard deviation in case of closing motion than in case of opening motion only for the low Swirl cylinder head, there is no preference in case of high Swirl cylinder head. However the relative standard deviation is always lower or equal to 10%. Looking at the relative standard deviation of the Flow Coefficient it is possible to notice that it is always in the order of magnitude of 10^{-3}, hence very small respect to the one of the Swirl Number. Due to this difference the FLow Coefficient results want affect the further step of the study.

Given the result reported above, the best setup to proceed with are bypass positions 0.8 and 1.1.

Table 7.1: Swirl Number relative standard deviation form stationary test results - High Swirl Number cylinder head

Bypass	0.5	0.8	1.1	1.4
std dev 0-15 mm	4%	3%	6%	6%
std dev 15-0 mm	10%	5%	4%	3%
Mean std dev	8%	8%	5%	4%

Table 7.2: Swirl Number relative standard deviation form stationary test results - Low Swirl Number cylinder head

Bypass	0.5	0.8	1.1	1.4
std dev 0-15 mm	5%	3%	4%	6%
std dev 15-0 mm	2%	3%	2%	3%
std dev cycle	4%	4%	3%	4%

Table 7.3: Flow coefficient relative standard deviation form stationary test results - High Swirl Number cylinder head

Bypass	0.5	0.8	1.1	1.4
std dev 0-15 mm	0.05%	0.19%	0.11%	0.18%
std dev 15-0 mm	0.10%	0.06%	0.17%	0.33%
Mean std dev	0.08%	0.08%	0.15%	0.26%

Table 7.4: Flow coefficient relative standard deviation form stationary test results - Low Swirl Number cylinder head

Bypass	0.5	0.8	1.1	1.4
std dev 0-15 mm	0.25%	0.05%	0.15%	0.31%
std dev 15-0 mm	0.25%	0.25%	0.25%	0.25%
std dev cycle	0.25%	0.13%	0.20%	0.26%

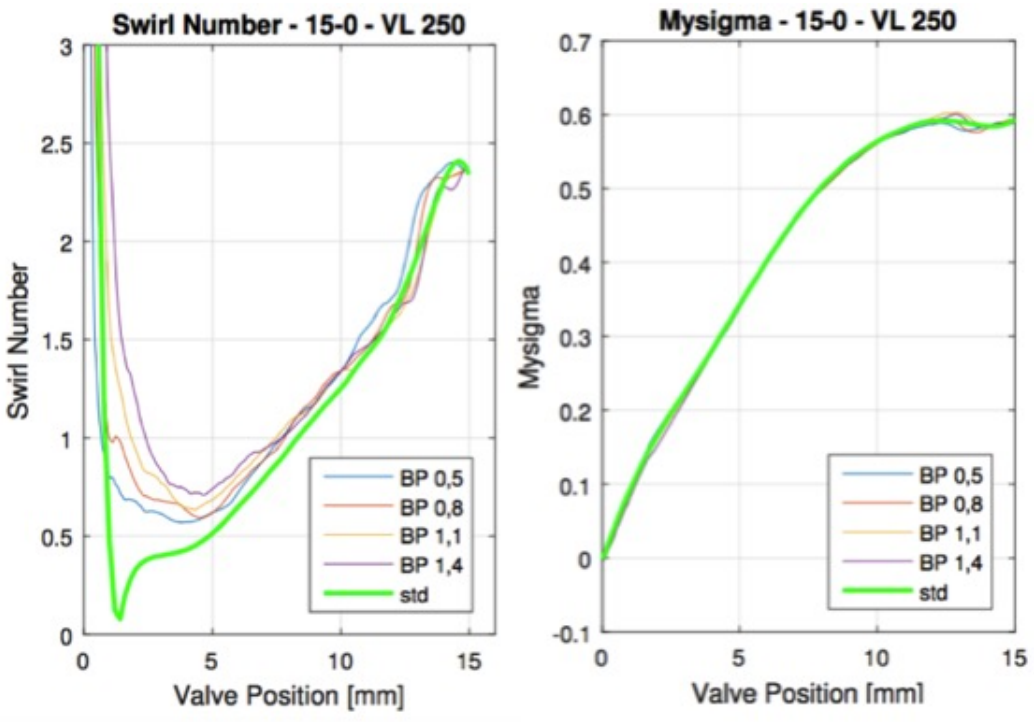

FIGURE 7.2: Swirl Number and $\mu\sigma$ Coefficient for high Swirl cylinder head in the closing motion for vale lift speed 250

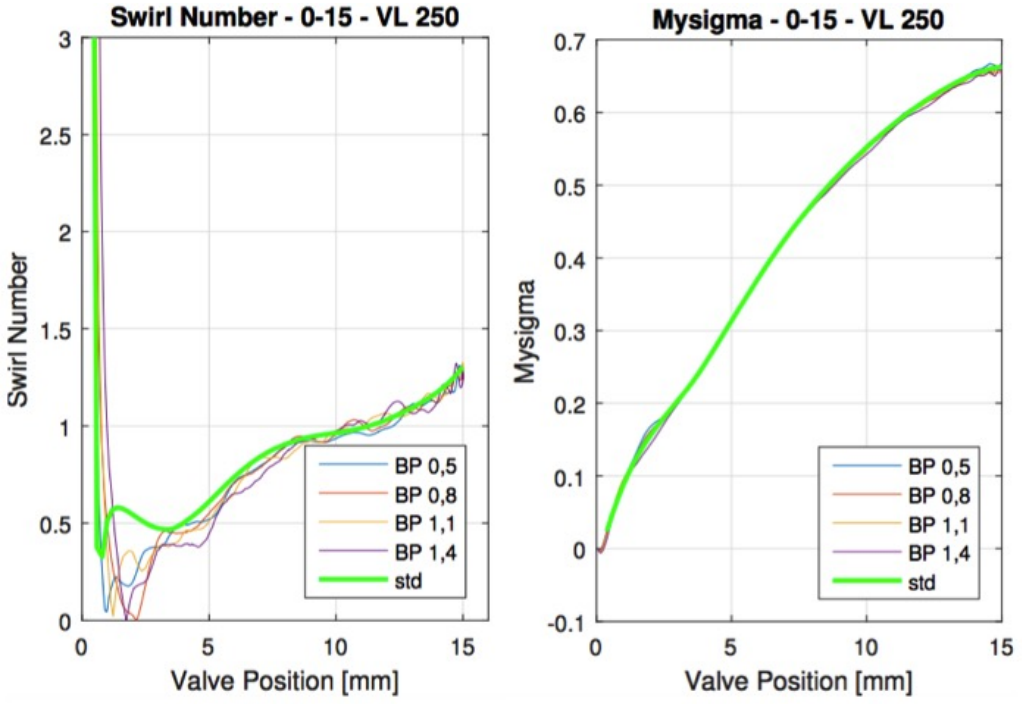

FIGURE 7.3: Swirl Number and $\mu\sigma$ Coefficient for low Swirl cylinder head in the opening motion for vale lift speed 250
Where in green is reporter the standard results obtained with 15 lift steps between 1 mm and 15 mm and the other colors represent different bypass position.

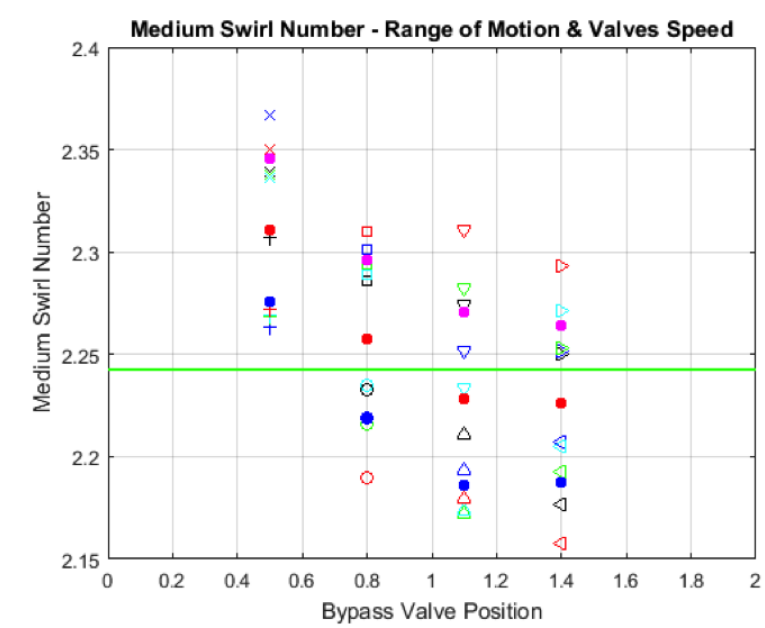

FIGURE 7.4: Medium Swirl Number comparison for high Swirl cylinder head

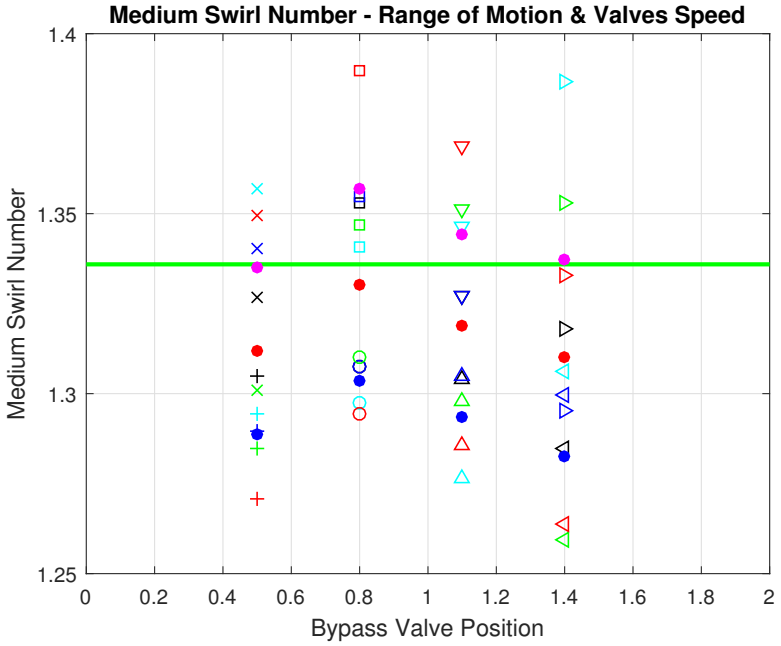

FIGURE 7.5: Medium Swirl Number comparison for low Swirl cylinder head
Where in green is reported the standard result, in red the mean result of the continuous tests, in pink the mean result of the closing range, in blue the mean result of the opening range and with equal symbols equal range of motion and with same colors same valve lift velocities

7.4 Repeatability Tests

Given the results of the *Setup Definition Tests* (7.3) the *Repeatability Tests* were performed 10 times with bypass valve positions 0.8 and 1.1, in both range of motion and with different valve lift velocity.

Figures 7.6 and 7.7 show the instantaneous Swirl Number and the instantaneous Flow Coefficient. Looking at the $\mu\sigma$ Coefficient it seems that the tests are highly repeatable, however looking at the Swirl Number it is evident that some repetition will be needed.

Tables 7.5, 7.6, 7.7 and 7.8 report the relative standard deviation from the stationary results of Swirl Number and Flow Coefficient, for both high and low Swirl Number cylinder head, respectively. The suggestion that derives from the results of this stage is that the best setup for high Swirl Number cylinder head is bypass 0.8 and opening motion of the valves, while there is no particular indication for the low Swirl Number cylinder head. As previously reported the relative standard deviation of the Flow Coefficient is of the order of magnitude of 10^{-3}, smaller than the relative standard deviation for the Swirl Number.

TABLE 7.5: Swirl Number relative standard deviation form stationary test results - High Swirl cylinder head

Bypass	0.8	1.1
std dev 0-15 mm	1%	6%
std dev 15-0 mm	1%	8%

TABLE 7.6: Swirl Number relative standard deviation form stationary test results - Low Swirl cylinder head

Bypass	0.8	1.1
std dev 0-15 mm	2%	4%
std dev 15-0 mm	5%	3%

TABLE 7.7: Flow coefficient relative standard deviation form stationary test results - High Swirl cylinder head

Bypass	0.8	1.1
std dev 0-15 mm	0.38%	0.38%
std dev 15-0 mm	0.63%	0.50%

TABLE 7.8: Flow coefficient relative standard deviation form stationary test results - Low Swirl cylinder head

Bypass	0.8	1.1
std dev 0-15 mm	0.24%	0.12%
std dev 15-0 mm	0.19%	0.12%

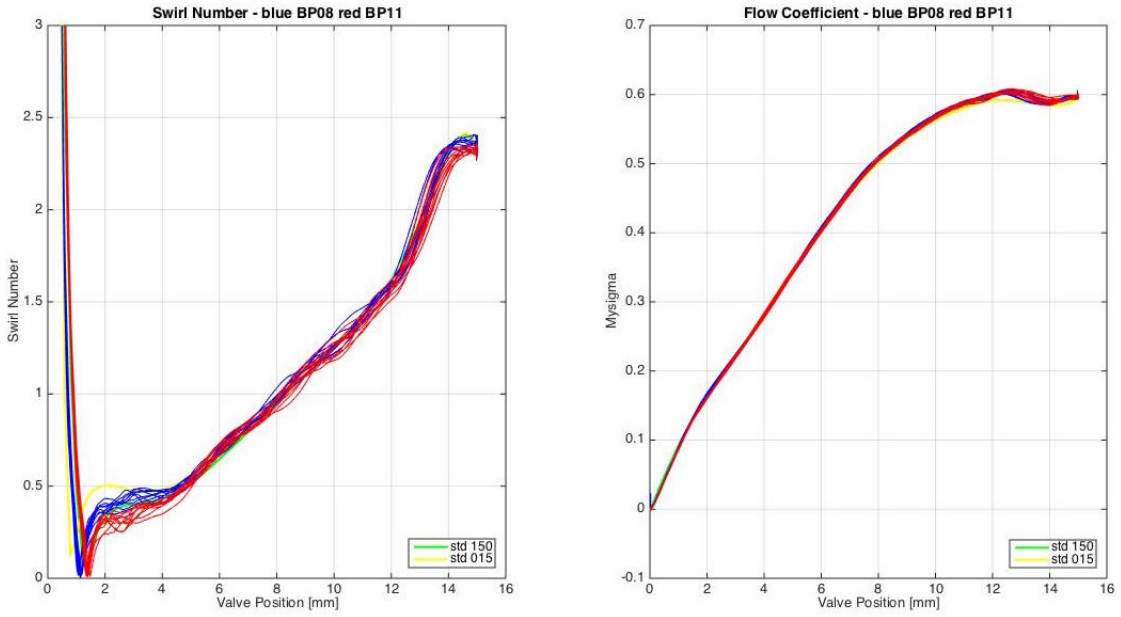

FIGURE 7.6: Main parameters
Where in yellow and green are reported the standard results, in red the result from the continuous test with bypass position 1.1 and in blue with bypass position 0.8

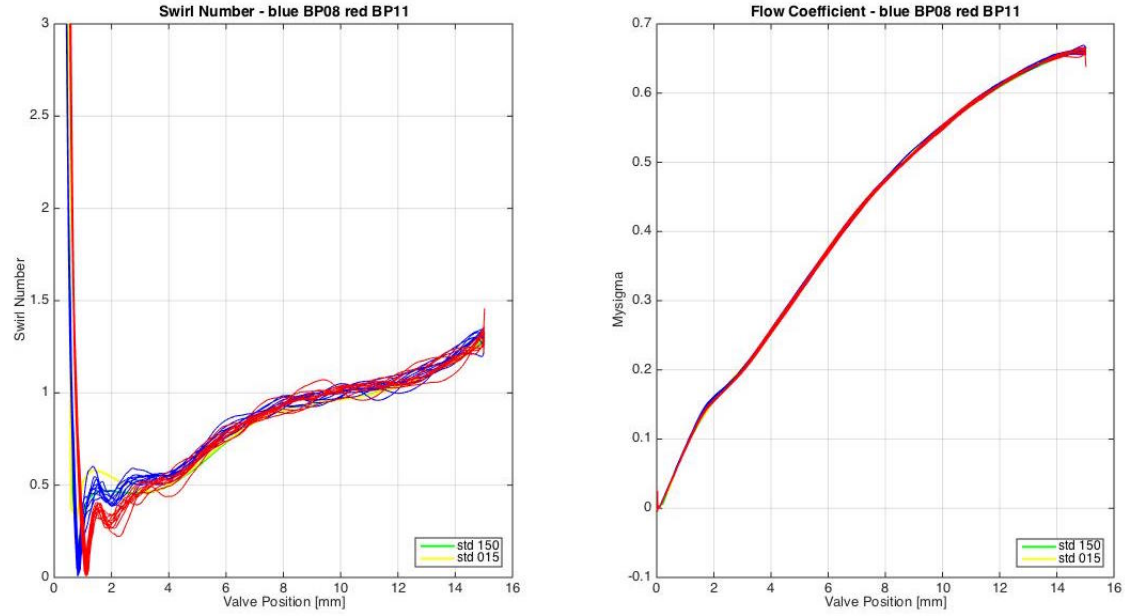

FIGURE 7.7: Main parameters
Where in yellow and green are reported the standard results, in red the result from the continuous test with bypass position 1.1 and in blue with bypass position 0.8

7.5 5 Cycles Tests

From the previous Section it seems that some repetition will be needed. However, repeating tests acquiring only in one range of motion means to wast half of the test time. Consequently it was investigate the possibility of repeated cycle (5) acquisition in both range of motions.

Tables 7.9 and 7.10 reports the medium Swirl Number result, while Tables 7.11 and 7.12 report the relative standard deviation of the Flow Coefficient. The $\mu\sigma$ Coefficient is always close to the stationary result (order of magnitude of relative standard deviation 10^{-3}). The Swirl Number relative standard deviation is lower in case of bypass 0.8 respect to the bypass 1.1.

Thus, acquiring in both range of motion does not seem to affect negatively the results.

TABLE 7.9: Swirl Number mean result and relative standard deviation from stationary test results - High Swirl cylinder head

Bypass	0.8		1.1	
Cycle time [s]	N mean	N std dev	N mean	N std dev
40 sec/cycle	2.18	7%	2.11	15%
50 sec/cycle	2.18	8%	2.11	13%
60 sec/cycle	2.17	6%	2.11	13%

TABLE 7.10: Swirl Number mean result and relative standard deviation from stationary test results - Low Swirl cylinder head

Bypass	0.8		1.1	
Cycle time [s]	N mean	N std dev	N mean	N std dev
40 sec/cycle	1.30	3%	1.28	6%
50 sec/cycle	1.30	3%	1.29	3%
60 sec/cycle	1.30	3%	1.29	3%

TABLE 7.11: Flow coefficient relative standard deviation from stationary test results - High Swirl cylinder head

Bypass	0.8	1.1
Cycle time [s]	$\mu\sigma$ std dev	$\mu\sigma$ std dev
40 sec/cycle	0.38%	0.29%
50 sec/cycle	0.35%	0.21%
60 sec/cycle	0.33%	0.25%

TABLE 7.12: Flow coefficient relative standard deviation from stationary test results - Low Swirl cylinder head

Bypass	0.8	1.1
Cycle time [s]	$\mu\sigma$ std dev	$\mu\sigma$ std dev
40 sec/cycle	0.02%	0.20%
50 sec/cycle	0.02%	0.20%
60 sec/cycle	0.02%	0.20%

7.6 40 Cycles Test

To define the number of cycle useful to reach a stable result both bypass positions (0.8 and 1.1) were investigated for about 40 cycles. The results seem to be the same for both cylinder heads: bypass position 0.8 is better than the one at 1.1.

From Figures 7.8 and 7.9 it is possible to see that an acceptable result can be reached using around ten cycles. Considering ten cycles at valve lift velocity 300 (as in this case) it means that the test will produce useful results in about 10 minutes.

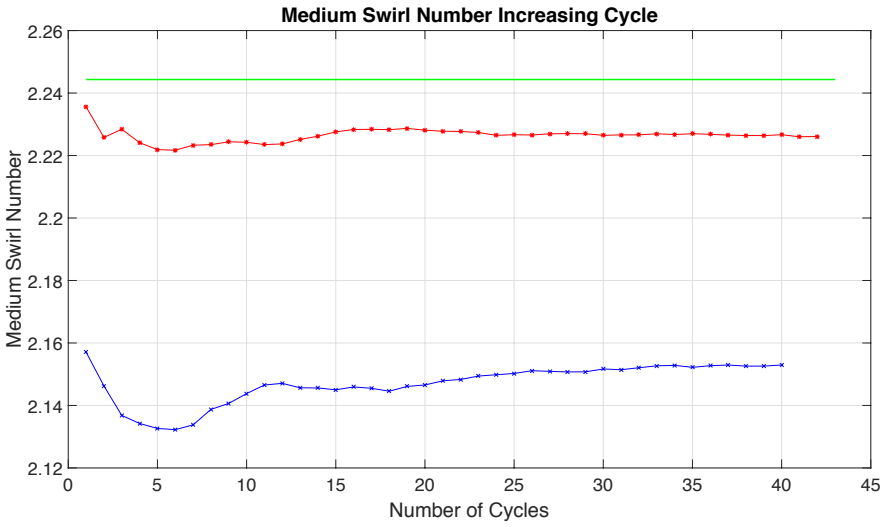

FIGURE 7.8: Medium Swirl Number increasing number of cycles comparison

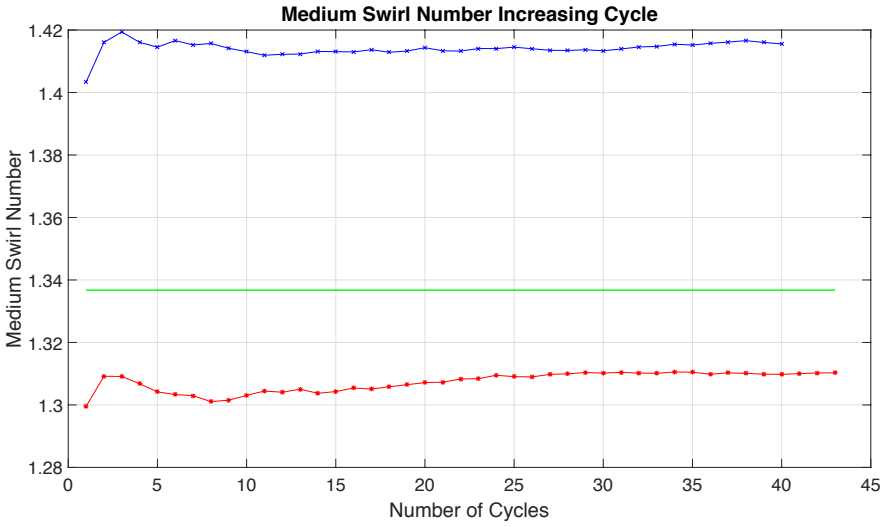

FIGURE 7.9: Medium Swirl Number increasing number of cycles comparison Where in blue are reported the result obtained with bypass 1.1, in red are reported the ones obtained with bypass 0.8 and in green is reported the result of the stationary test

7.7 Summary

From the complete series of tests, starting to the tests performed in order to determine the setup to the ones performed in order to define the correct number of cycles to get stable mean results, the same conclusion can be taken for both high and low Swirl Number reference cylinder head.

The best set up in order to reach results closer to the stationary ones is given by:

- bypass valve position 0.8;
- valve lift velocity 300;
- 10 repeated cycles (test time around 10 minutes).

Chapter 8

Flow Inertia Effect

Continuous motion of the valves will probably generate an inertia effect that needs to be investigated. Even if the mean results obtained from the experimental tests reported in Chapter 7 do not show any important variation from the stationary test, this *Chapter* will report the flow inertia investigation conducted on the experimental setup chosen in Chapter 7.

8.1 Study Procedures

To perform the study on the flow inertia effect was chosen as test sample the experimental data from a cyclic test previously conducted with the final setup chosen for the continuous test: bypass valve position 0.8 and valve lifter velocity 300. Inertia effect can be seen in variables directly acquired during the test, such as the volume flow rate, the pressure drop over the cylinder and the torque.

8.2 Analysis Results

8.2.1 Volume Flow

The previous investigation on the hydraulic head does not show any evidence of inertia, but some can be hidden by the flat bottom of the graph, due to the constant inlet area around cam angle 180°. Another parameter that can be useful to determine the inertia effect, by means of hysteresis, on the flow is the volume flow, directly computed in the test post process evaluation using the calibration map created in Chapter 4.

As show in Figure 8.1, hysteresis is present in each case. Moreover it is possible to notice that higher the valve lifter velocity, the higher the hysteresis in the volume flow rate and the higher the inertia effect on the flow. The hysteresis is given by the fact that it is more difficult to accelerate the flow rather than decelerate it.

In the opening motion (in Figure 8.1 the bottom lines), when the flow needs to be accelerated, the inertia and the friction of the flow meter work both against the

acceleration. Instead during the closing motion (in Figure 8.1 the upper lines) the inertia and the friction of the flow meter work together to decelerate the flow.

The inertia effect is visible from 2-12 mm lift, considering the fastest valve lifter velocity (400), the distance is covered in 14 sec. Given the acquisition frequency of 10 Hz, in 14 sec are acquired about 140 samples. Then it is possible to consider the actual acquisition frequency high enough to obtain good time resolution.

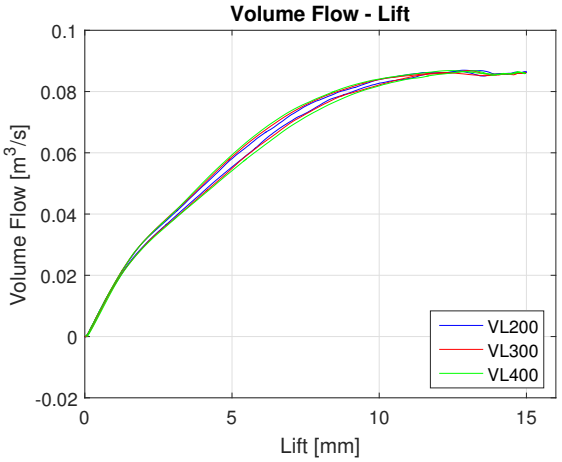

FIGURE 8.1: Volume flow rate for different valves lifter velocities

8.2.2 Pressure Drop Over The Cylinder

Inertia effect can be visible also in the pressure drop over the cylinder. Then the raw data is plotted over the lift (Figure 8.2) and hysteresis is noticeable: higher the valve lifter velocity larger the hysteresis. This suggest, as in the case of the volume flow, that the inertia effect increase increasing the valve velocity.

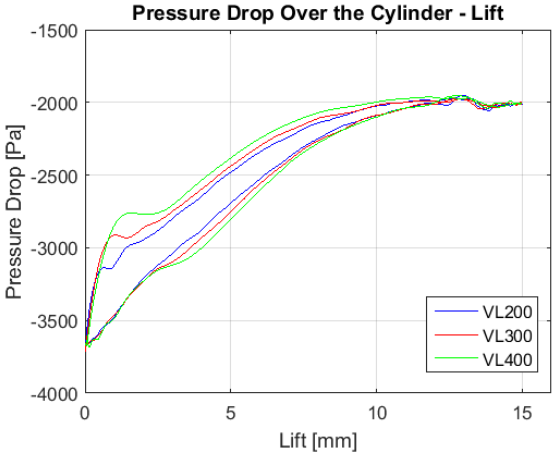

FIGURE 8.2: Pressure drop over the cylinder as function of the lift

8.2.3 Torque

To complete the inertia analysis of the parameters used to compute Swirl Number and Flow Coefficient, the Torque was analyzed as done with the volume flow and pressure drop over the cylinder in the previous Sections.

Figure 8.3 shows the same behaviour previously expressed for both pressure drop and volume flow: the higher the valve lifter velocity the larger the hysteresis. In this case is also possible to notice that for lower valve velocity the Torque has larger fluctuation with respect to the case of high valve velocity.

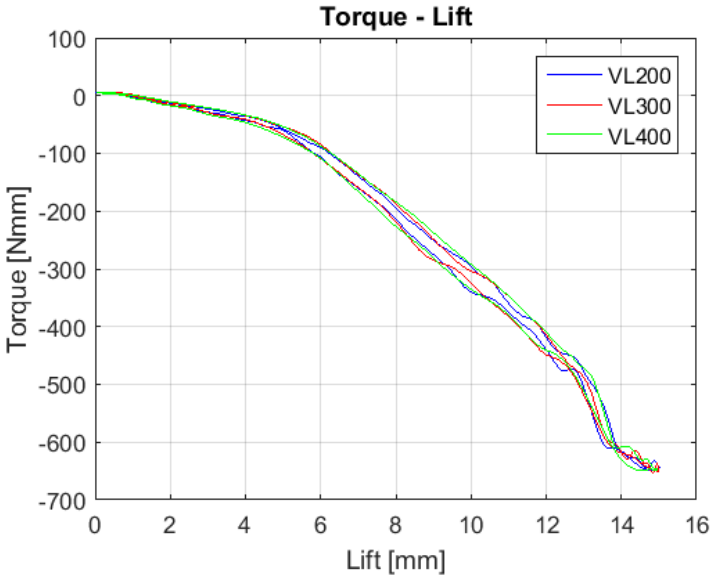

FIGURE 8.3: Torque for different valves lifter velocities

8.3 Summary

Inertia effect is present and affect the flow as shown in the previous Sections. However this inertia can be caused by the time response of flow meter (that has mechanical inertia). Whatever the inertia is caused by the mechanical inertia of the flow meter or by the motion of the inlet valves, it does not affect to much the mean result, as show in Chapter 7.

Chapter 9

Axial Velocity Distribution in the Cylinder

This *Chapter* reports measurements and analysis of the axial velocity in the cylinder both for stationary and continuous test conditions. The measurements were performed using backscatter *Laser Doppler Anemometry (LDA)* (or Laser Doppler Velocimetry, LDV).

9.1 Laser Doppler Anemometry Theory

Laser Doppler Anemometry is a non-intrusive method to measure the flow velocity, by measurement of the velocity of small particles that are following the flow. A two beam LDA system is capable to measure the velocity in a specific direction in a single point of the flow field. The LDA does not require calibration and it has, when properly set, high temporal and spatial resolution. The measurement point is the volume created by the intersection of two laser beams, the smaller the volume of intersection the higher the spatial resolution of the acquired data. The velocity is determined through the Doppler effect, i.e. the frequency shift of the scattered light from the moving tracer particles.

9.1.1 Laser Beams, Transmitting Optics and Measurement Volume

The LDA system used was the *DANTEC FlowLite system*, for a schematic see Figure 9.1. In the main unit the laser beam is divided into two beams by the beam splitter and one of them is frequency shifted by the Bragg cell. A fibre optical cable is

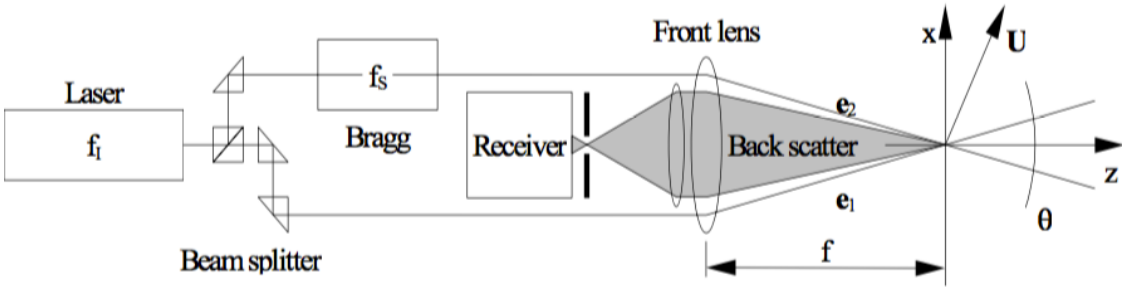

FIGURE 9.1: Backscatter LDA transmitting optics. From [5]

used to guide the laser light from the main unit to the probe head where the lens system focusses the two laser beams into the intersection point, i.e. measurement volume. The probe head also collects the scattered light and directs it back through the fibre optical cable to the main unit where it is detected by a photomultiplier.

9.1.2 Doppler Effect

The principle of the Laser Doppler Anemometry can be explained by looking at the interference pattern created by the two intersecting laser beams in the measurement volume, see Figure 9.2. If a particle moves through this interference pattern it will scatter a 'blink' every time when it passes a white line. This gives rise to a burst of blinks in the receiving photomultiplier and by determining the time between the peaks in the burst the velocity of the particle can be found if the distance between the lines in the measurement volume is known. This distance is determined from the laser wave length (λ) and the angle (θ) between the beams and becomes $\Delta x = \lambda/2 \cdot \sin(\theta/2)$.

A particle that passes through the measurement volume gives rise to a burst with a Doppler frequency (f_D). From that frequency the velocity perpendicular to the fringe pattern can be calculated as

$$u_x = \frac{\lambda}{2 \cdot \sin(\theta/2)} \cdot f_D \tag{9.1}$$

However as can be seen this does not allow the system to determine the flow direction of the particle and therefore one of the laser beams is shifted in frequency with the Bragg cell which gives rise to a moving fringe pattern. If the velocity of the

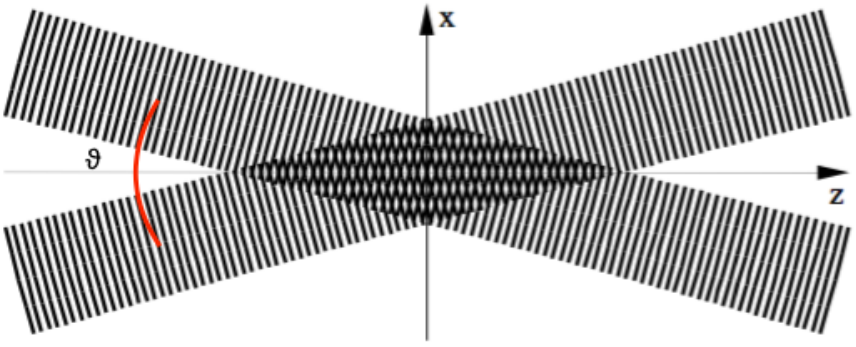

FIGURE 9.2: Beams intersection and axes in LDA setup. From [5]

fringes is higher than the highest velocity of the particles all particles will have a velocity bias that can be subtracted from the inferred velocity.

9.2 Experimental Setup and Procedure

As in Chapter 7 the series of tests were repeated with the same setup for both the high and low Swirl Number reference cylinder heads (4.2). In order to have optical access to inside of the cylinder the metal cylinder was replaced by a glass cylinder. The laser head was mounted on a traversing system so it could be moved in the vertical and horizontal directions and positioned such that it measures the axial (vertical) velocity. In this way it is possible to control the height (Z plane) and the horizontal position (radial position) of the measurement volume. To change the azimuthal position of the measurement volume with respect to the valves the cylinder head was rotated. A smoke machine was used to produce the tracer particles and the smoke machine was placed in the room and filled the room where the setup was located.

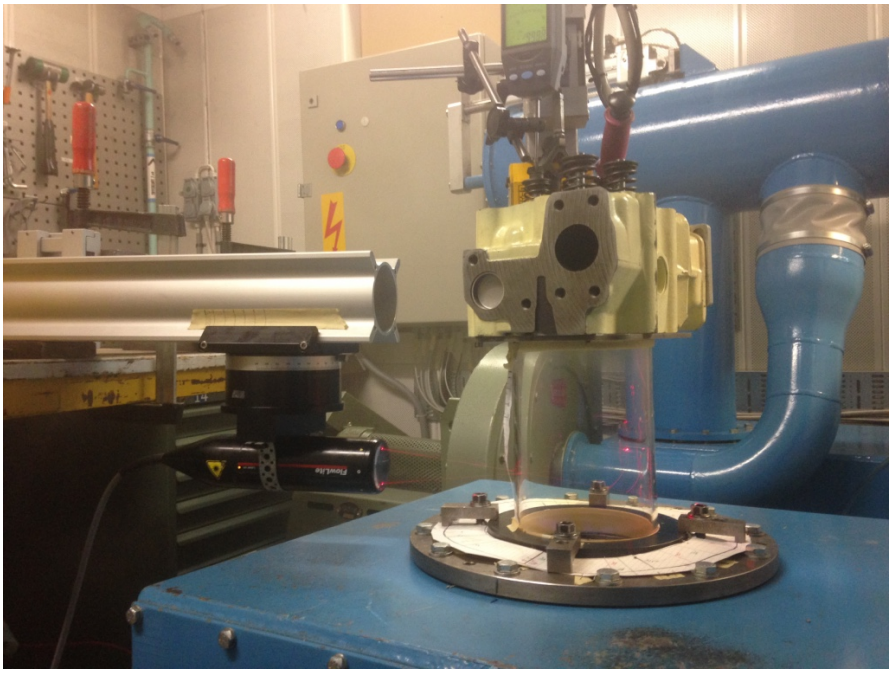

FIGURE 9.3: Example of measurement in the bottom Z plane

Prior to performing the experimental tests it was necessary to do preliminary tests to establish the right amount of smoke to be used during the tests and the right setup for every parameter of the *BSA Flow Software* (Figure 9.4), such as sensitivity, signal gain and burst detector SNR level, to get the desired compromise between the data rate and the validation and also a good Doppler burst signal.

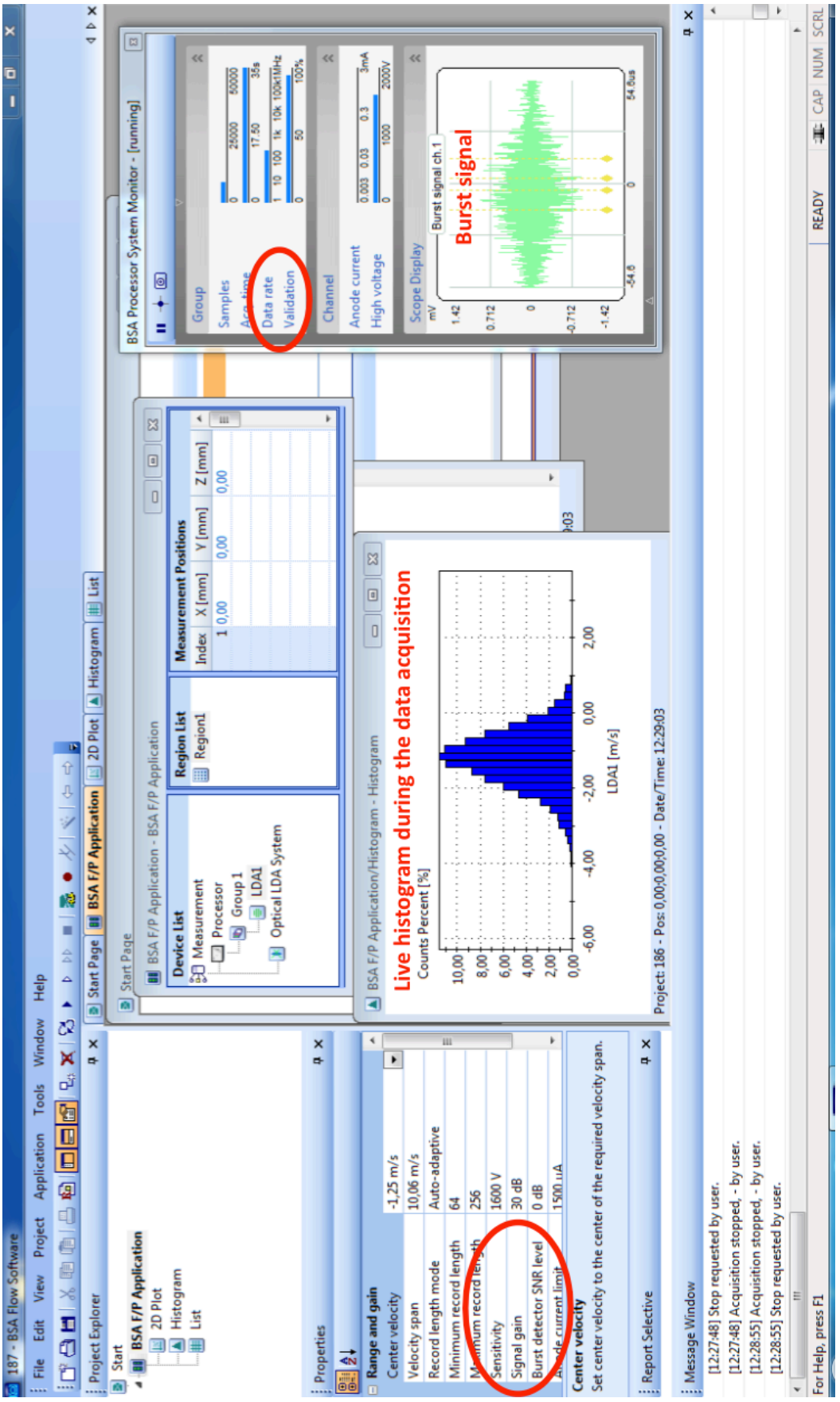

FIGURE 9.4: BSA Flow Software panel

The series of tests to study the flow pattern variations were performed at two different heights from the honeycomb matrix and considering 41 points on the cylinder surface. The Z planes were chosen one at the bottom and one at the top of the cylinder, respectively at 80 mm and 185 mm from the honeycomb as show in Figure 9.5. The location of the planes was chosen considering that it was not possible to measure below 85 mm and above 185 mm because the interference between laser beams due to limited optical access. The internal point were chosen following different θ grid depending on the radial position (Figure 9.6) as reported in Table 9.1.

The measurements were made for two stationary lift, 10 mm and 15 mm, and for the non-stationary case with valves moving in cycle 10-15-10 mm.

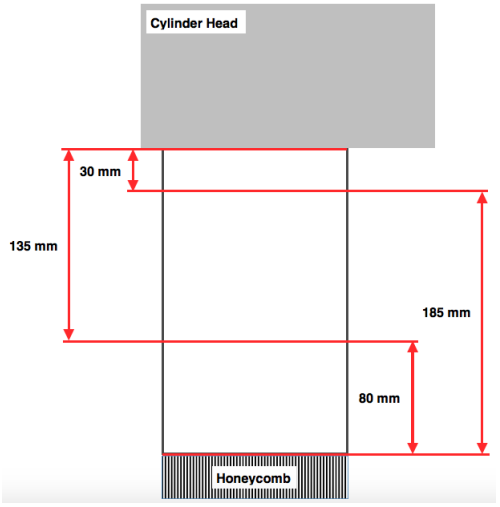

FIGURE 9.5: Z planes scheme

TABLE 9.1: Grid point distribution for LDA measurements

Radius	θ **Steps**
mm	deg
60	30
48	36
36	45
24	60
12	90
0	0

9.2.1 Evaluation Method

For every point acquired the signal were re-sampled to evaluate them with constant acquisition frequency. This frequency was chosen as the mean acquisition frequency during the test itself. The data were analysed in three different ways

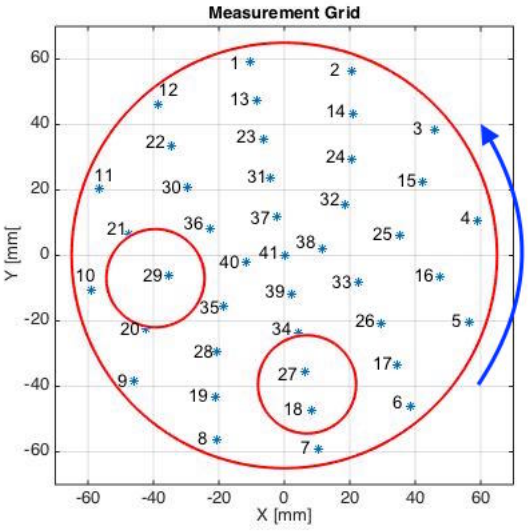

FIGURE 9.6: Measurement grid

- Contour plots of the vertical velocity of the two different Z planes were computed
- the probability density function (PDF) at each position was evaluated
- the fast Fourier transform (FFT) periodogram at each position was evaluated

However for the two last ways the moving valves case were excluded since result of FFT spectra and PDF of non stationary data are meaningless.

9.3 LDA Experimental Results

9.3.1 Flow Distribution in Z planes

The mean velocity distribution over the two Z planes (the bottom one at 80 mm and the upper one at 185 mm from the honeycomb matrix), are shown in Figure 9.7 for the high Swirl head and in Figure 9.8 for the low Swirl head. The three figures on the left is for $z = 80$ mm and the right column is for $z = 185$ mm. The upper row is for a valve lift of 10 mm, the middle row for a valve lift of 15 mm and the bottom row shows the moving valve case.

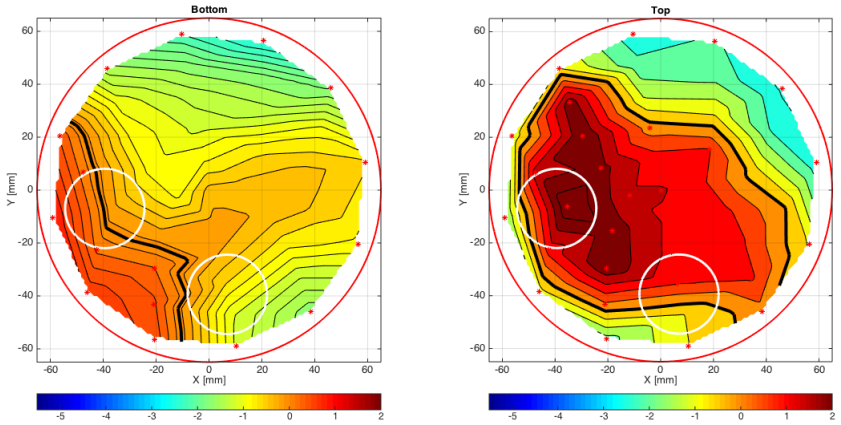

(a) 10 mm Lift

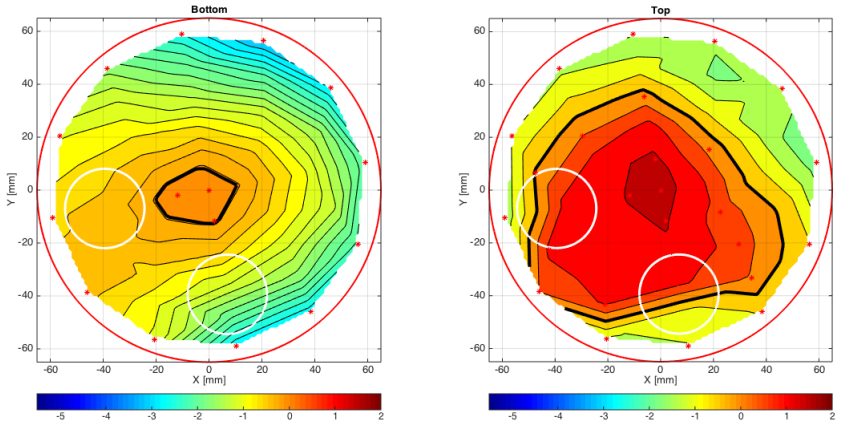

(b) 15 mm Lift

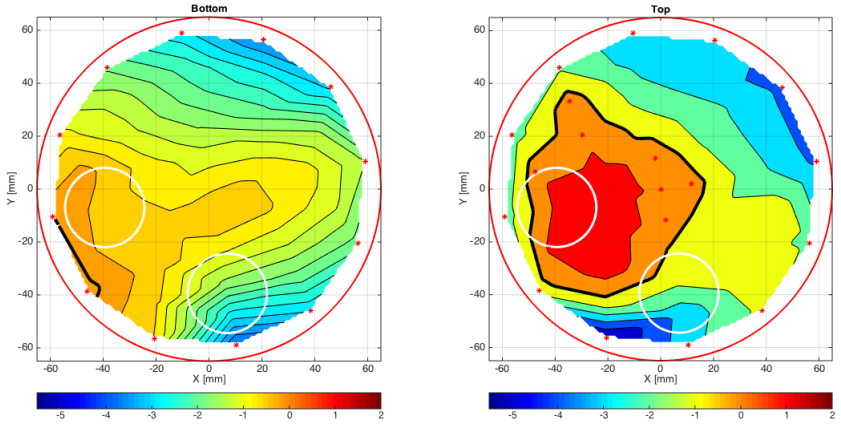

(c) Moving valves

FIGURE 9.7: High Swirl Number cylinder head mean axial velocity

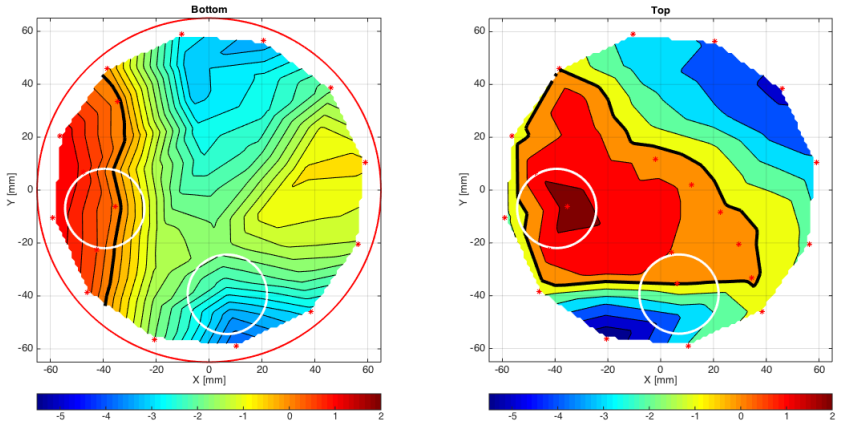

(a) 10 mm Lift

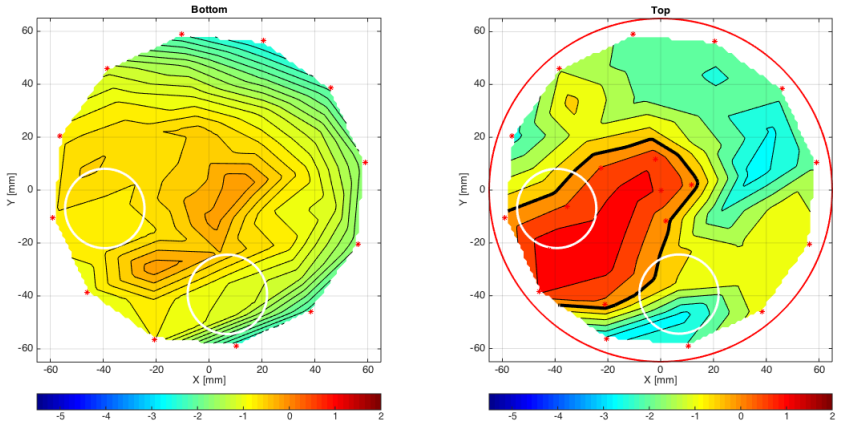

(b) 15 mm Lift

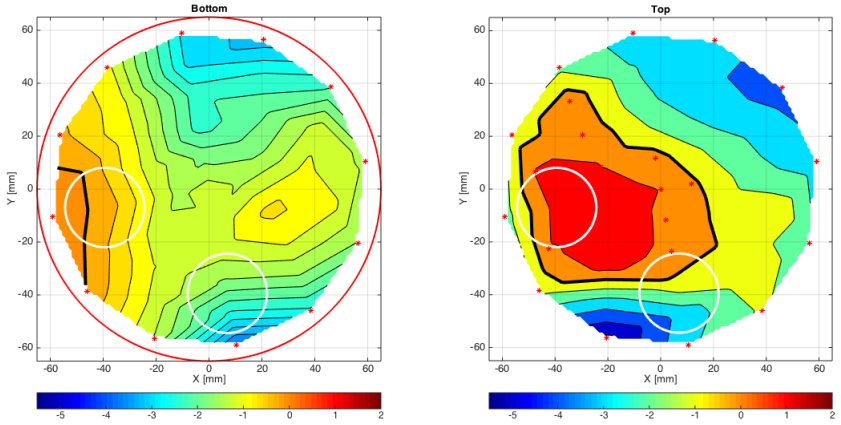

(c) Moving valves

FIGURE 9.8: Low Swirl Number cylinder head mean axial velocity

In the plots the contour line of zero axial velocity is marked with a thick black line, thereby clearly distinguishing the region of up flow from down flow in the cylinder. As can be expected the plots show that the down flow is concentrated to the side walls of the cylinder whereas there is an up flow in the central part, clearly indicating that there is a tumble motion in the cylinder. The tumble motion is stronger for 10 mm valve lift as compared to 15 mm, and as expected the positive axial velocity is much higher at the top plane. For the tumble motion there is not any major difference seen for the high and low Swirl heads. However no information of the swirling motion can be obtained from these measurements.

9.3.2 Example of PDF and spectra of the axial velocity

In the following Section we report some examples of the probability density function (PDF) and the fast Fourier transform (FFT) spectra for two specific measurement positions, one in each plane. For the high Swirl case we chose point number 25 for the upper Z plane, and for the bottom Z plane point number 5, see Figure 9.9.

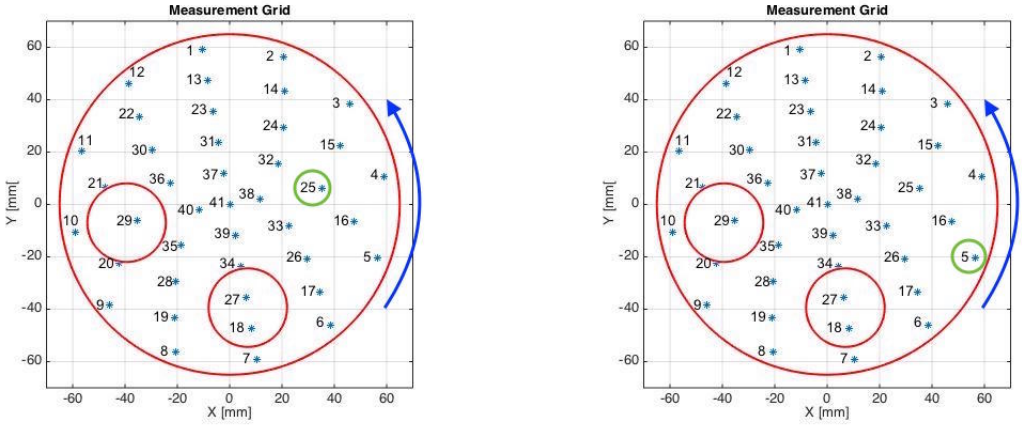

(a) Top plane

(b) Bottom plane

FIGURE 9.9: Measurement points for PDF and spectra

9.3.3 PDF Distribution Analysis

The PDFs shown in Figures 9.10 and 9.11 are quite smooth and show that the number of samples seems to be enough. The velocity distributions are quite different for the two valve lifts where for the 10 mm the velocity is mainly positive and for the 15 mm case it shows both positive and negative velocities.

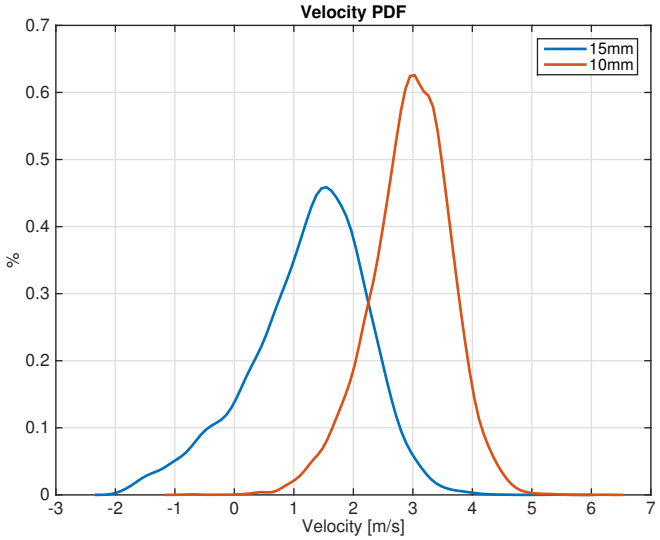

FIGURE 9.10: PDF for point 25 in the upper Z plane of the high Swirl cylinder head

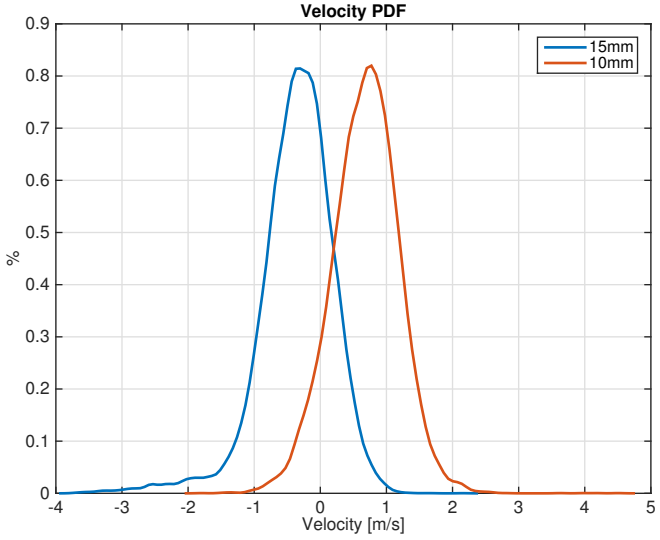

FIGURE 9.11: PDF for point 5 in the bottom Z plane of the high Swirl cylinder head Where in red is reported the 10 mm lift case while in blue the 15 mm lift case.

9.3.4 Spectral Analysis

From the FFT spectra analysis, examples for Z planes are reported in Figures 9.12 and 9.13, it is possible to see that for the 15 mm case, close to the valves in the top Z plane and almost everywhere in the bottom Z plane, there is an energy peak around 13 Hz, whereas in the 10 mm lift case the peak is present but it has lower amplitude.

For the low Swirl number case we present spectra from point number 2 for the upper Z plane and point number 7 for the bottom plane.The spectral analysis (Figures

9.14 and 9.15) shows once again an energy peak at 13 Hz similar to those from the high Swirl Number case but an higher level of energy.

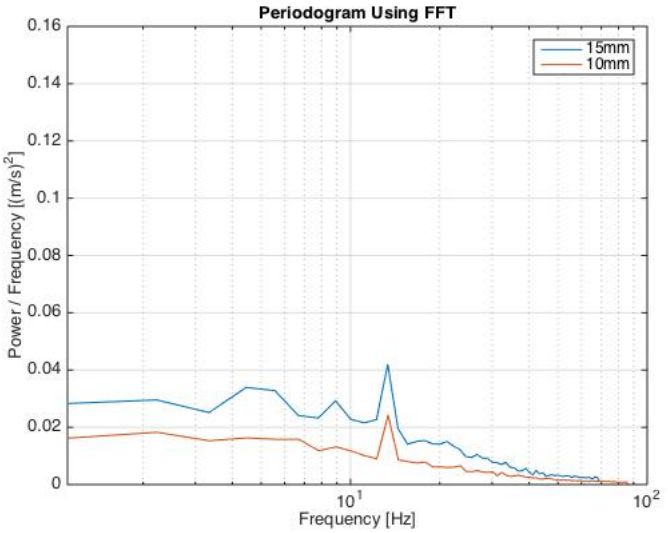

FIGURE 9.12: FFT Spectra for point 25 in the upper Z plane of the high Swirl cylinder head

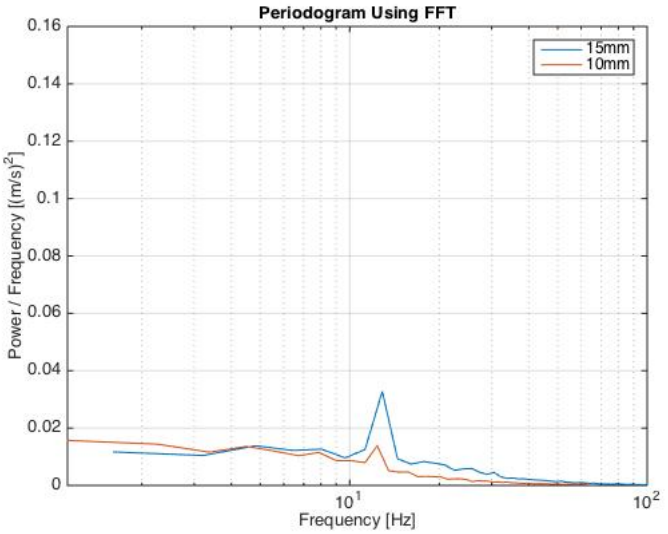

FIGURE 9.13: FFT Spectra for point 5 in the bottom Z plane of the high Swirl cylinder head
Where in red is reported the 10 mm lift case while in blue the 15 mm lift case.

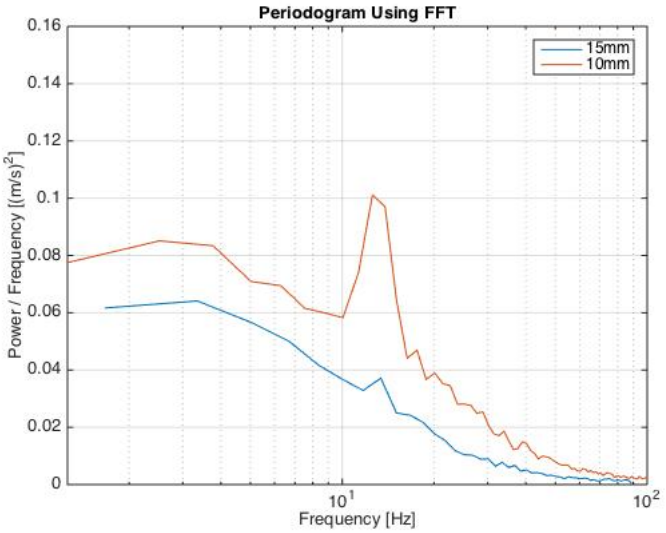

FIGURE 9.14: FFT Spectra for point 2 in the upper Z plane of the low Swirl cylinder head

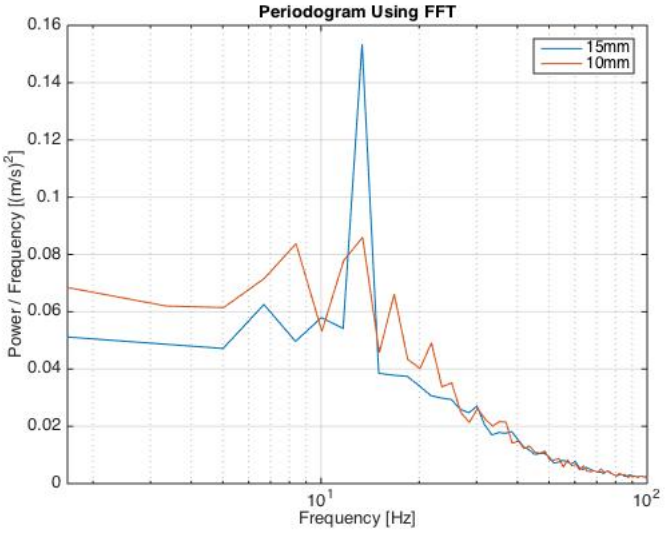

FIGURE 9.15: FFT Spectra for point 7 in the bottom Z plane of the low Swirl cylinder head
Where in red is reported the 10 mm lift case while in blue the 15 mm lift case.

9.4 Energy Peaks at 13 Hz

In this *Section* the energy peaks at 13 Hz, for both high and low Swirl Number reference cylinder heads will be discussed.

To verify the presence of the energy peak at 13 Hz, the raw data were filtered with running average (Figure 9.16 in green): around 13 peaks could be counted in 1 second,

confirming the 13 Hz frequency from the FFT.

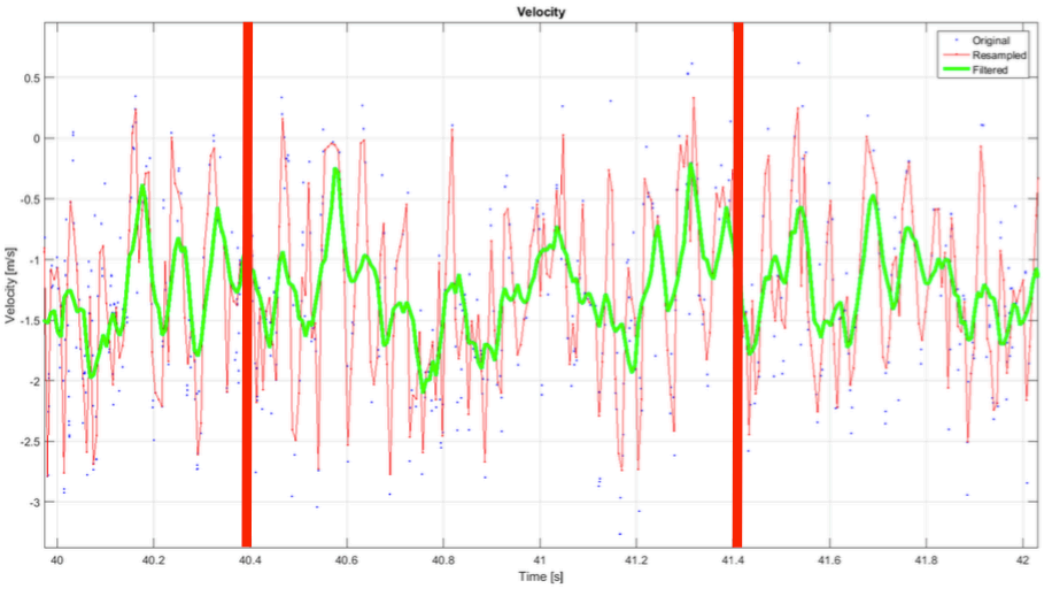

FIGURE 9.16: Filtered raw data to see the frequency of the signal for high Swirl head

To investigate the energy peaks in all the points studied, surface graphs with peaks magnitude were plotted for all the cases (10 mm lift, 15 mm lift, top and bottom Z planes). It is possible to notice that as seen in the spectral analysis the case mainly affected by the energy peak at 13 Hz is the 15 mm lift case and that at top Z plane the peaks are close to the inlet valves whereas at the bottom Z plane the peaks are distributed all over the surface.

To search for the source of the frequency peak the characteristic Strouhal Number (St) of the cylinder heads was assumed to be:

$$St = \frac{f \cdot D}{V} = 0.4 \tag{9.2}$$

where f is the frequency, D the characteristic dimension related to the frequency and V is the velocity in the same location as D.

The velocity at the inlet valves seat can be calculated using the volume flow, acquired in previous tests with the same setup of these tests, and using the valves seat area (minus the area of the valves stem). Considering the above mentioned parameters the velocity at the valves seat is 5.4 m/s. Therefore, given a Strouhal number of 0.4

and a velocity of 5.4 m/s, the dimension related to the investigated frequency is about 160 mm. This is close to both the diameter of the cylinder (130 mm) and the length of the cylinder which is 220 mm from the cylinder head to the honeycomb matrix.

Another possibility would be that the length of the inlet ports (116 mm) is associated with the energy peak. Further tests changing the setup will be needed to verify if the energy peaks will be still present and if they will have the same frequency (see Chapter 10). An additional investigation can also be performed in case of torque meter able to acquire at higher frequency, to study the presence of energy peaks in the torque measurements.

Moreover, even if it is not possible to define a spatial relation for the energy peaks, it is possible to notice (Figure 9.17) that the peaks are located in the same regions of small axial velocity gradients. In light of the above evaluation one possibility is to assume that the energy peaks at 13 Hz is related to the dynamics of the Swirl vortex inside the cylinder.

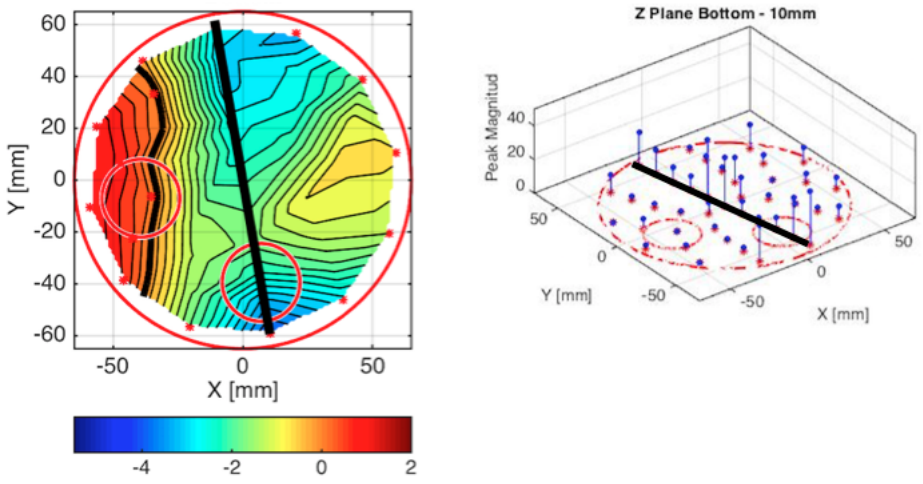

FIGURE 9.17: Relation between the 13 Hz peaks and velocity gradient for low Swirl Number cylinder head

Chapter 10

Energy Peak Investigation

This *Chapter* reports the investigation performed to study the energy peak at 13 Hz that was discovered in the results of the LDV tests in Chapter 9.

The hypothesis regarding the cause of the energy peak made at the end of the LDV experimentation are:

- Swirl vortex evolution in the cylinder diameter;
- Swirl vortex evolution in the cylinder length;
- intake port effect;

In the following *Sections* will be reported the results of the investigation regarding the cylinder length and the influence of the inlet port. Unfortunately there is no way to verify the effect of the cylinder diameter, due to the fact that there is no cylinder head available with different diameter. Furthermore, the effect of the energy peaks is searched in the torque parameter during stationary test and continuous ones.

10.1 Cylinder Effect - Experimental Procedure

In order to investigate the effect of the length of the cylinder a different glass cylinder, 635 mm long, was installed on the test bench. Because of the cylinder length and the provisional connection with the settling chamber, it was chosen to not use a real cylinder head, that weight around 20 kg and could have damaged the cylinder, but a much lighter air box with similar geometry was used instead. The setup for the investigation is visible in Figure 10.1.

The experimental points were chosen looking at the previous LDV results. The measurements were performed in the bottom plane, close to the honeycomb matrix, wall to wall perpendicularly to one inlet valve, for stationary valve lifts of 10 and 15 mm.

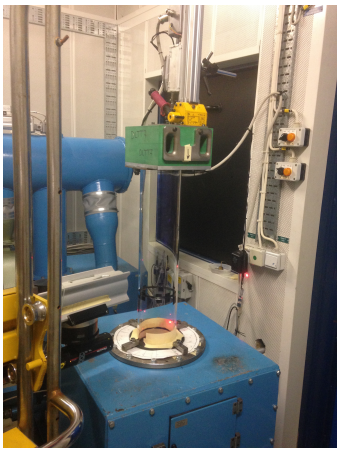

FIGURE 10.1: Setup for the experimental test with the long (635 mm) glass cylinder.

10.1.1 Experimental Results

For each set of data acquired from the experimental tests the spectral analysis was performed using, as done in Chapter 9, the Fast Fourier Transform (FFT) and dividing the time signal in subsets for which spectra were calculated and ensemble averaged to get a smooth spectrum.

With the exception of the central point in the cylinder, all experimental points show an energy peak around 13 Hz (Figure 10.2). The presence of the energy peak at this frequency shows that the hypothesis that frequency is related to the length of the cylinder is not correct.

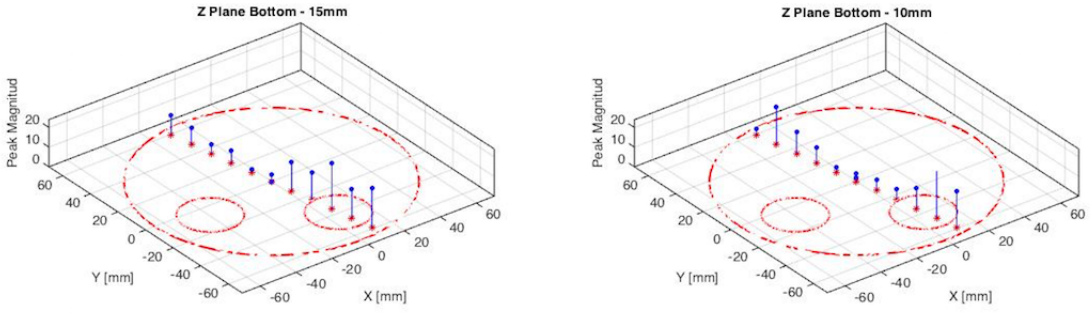

FIGURE 10.2: Energy peak magnitude - Cylinder length comparison

10.2 Intake Port Effects

To verify the effect of the inlet ports LDV tests were performed with valves at fixed positions, considering alternatively both valves and each single valve. To avoid damaging

the long glass cylinder the air box from the previous *Section* was used. However to verify the results also one single point for the high Swirl Number cylinder head was tested.

The experimental points for the air box are (Figure 10.3):

- valves lift 10 mm, Z plane close to the cylinder head, radius 60 mm and $\theta = 30°$;
- valves lift 10 mm, Z plane close to the cylinder head, radius 60 mm and $\theta = 150°$;
- valves lift 10 mm, Z plane 220 mm below the cylinder head (has the bottom plane from Chapter 9), radius 60 mm and $\theta = 0°$;
- valves lift 10 mm, Z plane 220 mm below the cylinder head (has the bottom plane from Chapter 9), radius 48 mm and $\theta = 180°$;

The experimental point for the high Swirl Number cylinder was for a valve lift of 15 mm, Z plane 220 mm below the cylinder head (has the bottom plane from Chapter 9), radius 60 mm and $\theta = 180°$;

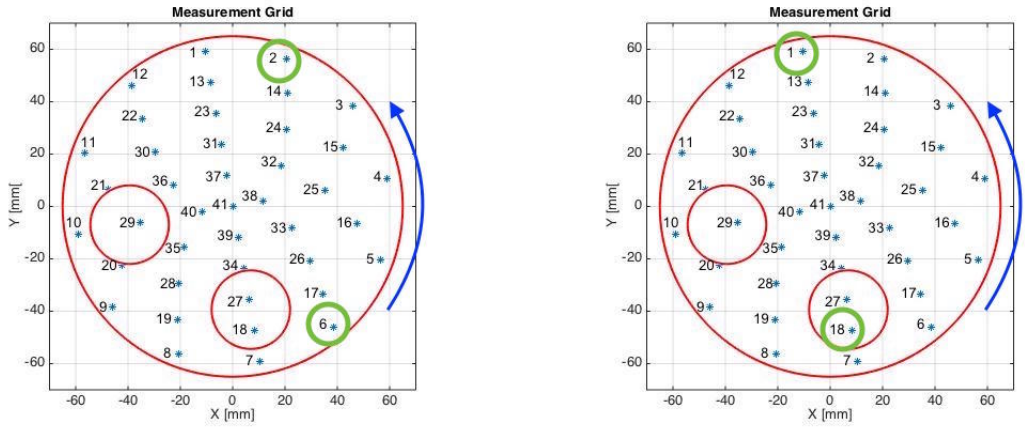

(a) Top plane

(b) Bottom plane

FIGURE 10.3: Air box tests experimental point

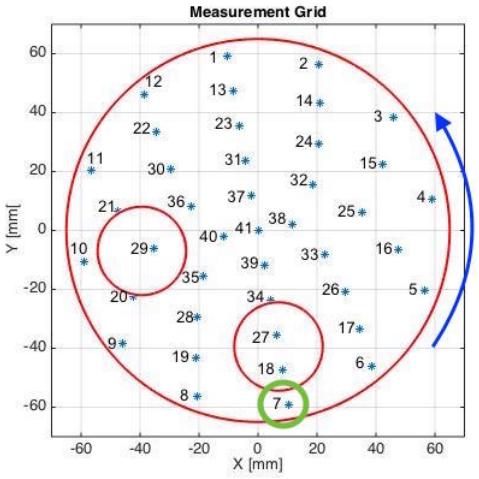

FIGURE 10.4: High Swirl Number cylinder head test experimental point

10.2.1 Experimental Results

The series of test, with both air box and real cylinder head, show the same behaviour: in the majority of the cases the energy peak at 13 Hz is present for the tests performed with both inlet valves opened while there is no peak in the cases regarding one single valve opened (Figure 10.5 shows an example from the test with the air box). However in some cases the energy peak is present also in the case of one single valve opened (either one of the two, without preference), even if with lower magnitude compared to the case with both (as in Figure 10.6).

The hypothesis of some inlet ports effect is strongly supported by these results. However further tests are needed to fully understand this effect.

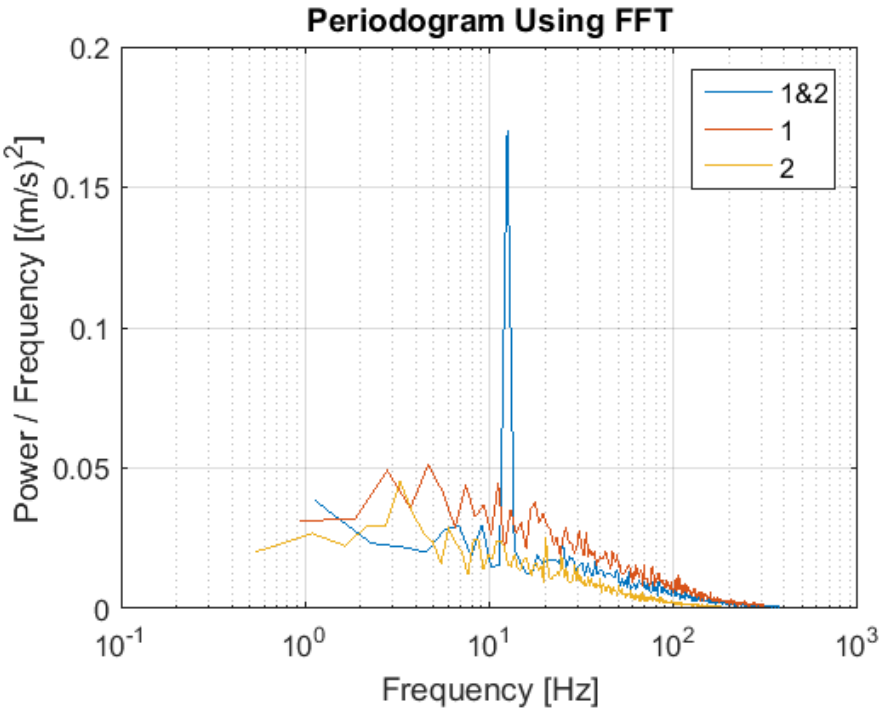

FIGURE 10.5: FFT spectra - Air box, top plane, second point

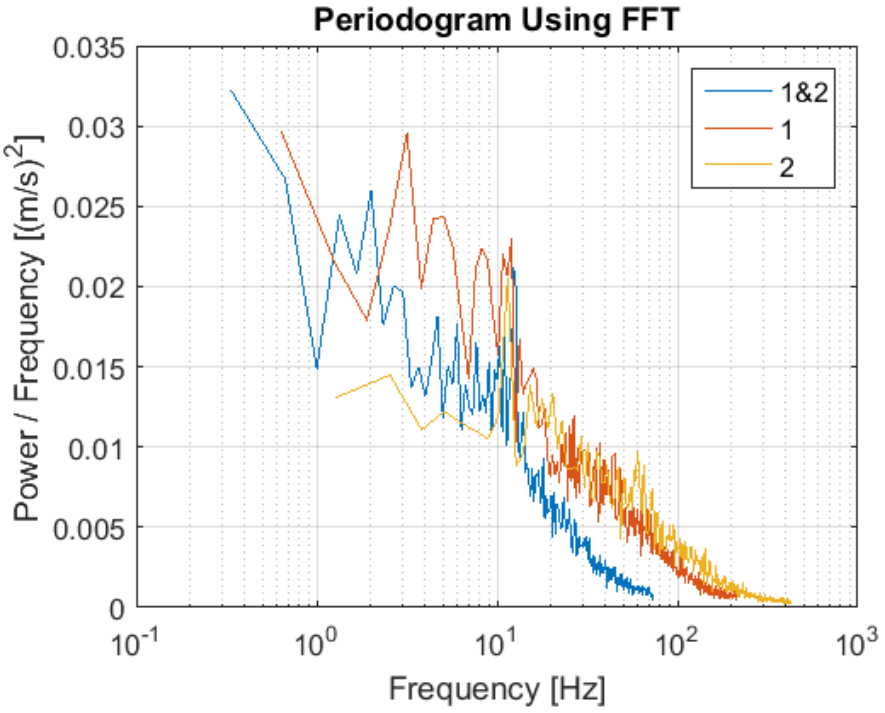

FIGURE 10.6: FFT spectra - Air box, top plane, first point

10.3 Effect Of The Energy Peak On The Torque

To investigate the frequency peak at 13 Hz found in the spectral analysis of the flow velocity the acquisition frequency of the torque meter was increased to 2500 Hz. Tests were performed step-by-step to consider every possible effect:

- Rig turned off;
- Rig in starting phase;
- Rig running without cylinder head;
- Rig running without cylinder and cylinder head;
- Comparison of three valves lift positions in the low Swirl Number reference cylinder head.

The data acquired during the starting phase of the rig, the ones acquired without the cylinder and the cylinder head show high level of energy at very low frequency, hence in frequency below 10 Hz will be considered as caused by mechanical vibration of the rig.

Stationary test were performed for the low Swirl Number reference cylinder head. For each valves lift step the torque was acquired at 2500 Hz each time for 30 sec. In Figure 10.7 are reported the comparison graph for 5, 10 and 15 mm lift for each cylinder head. It is possible to notice that there are some effect in between 5 and 15 Hz.

To conclude the energy peaks around 10 Hz discovered are probably the combination of the evolution of the flow inside the cylinder and the geometry of the cylinder head.

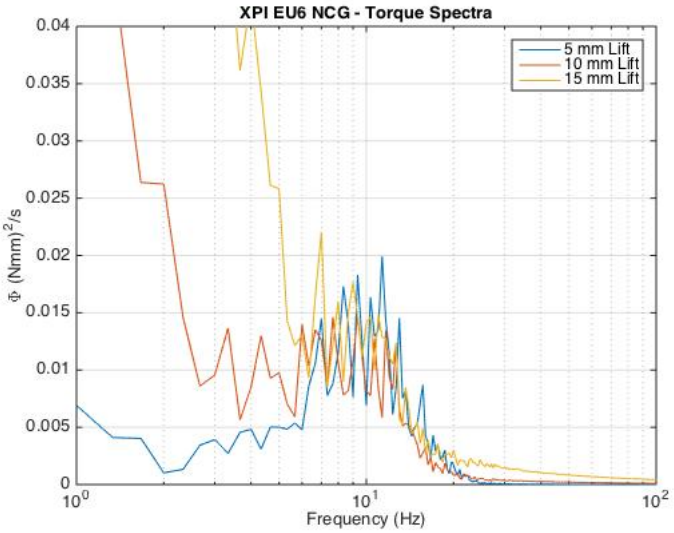

FIGURE 10.7: Torque spectrum comparison for 5, 10 and 15 mm lift

10.3.1 Continuous Test Results

Once again, it is not possible to compute the spectral analysis in the case of non stationary data. Therefore for the continuous cases the only analysis will be performed on the time signal. As shown in Figure 10.8, the behaviour of the torque meter is the same when considering the same range of motion. The time response of the torque meter, given the human error during the acquisition, seems to be enough to follow the flow.

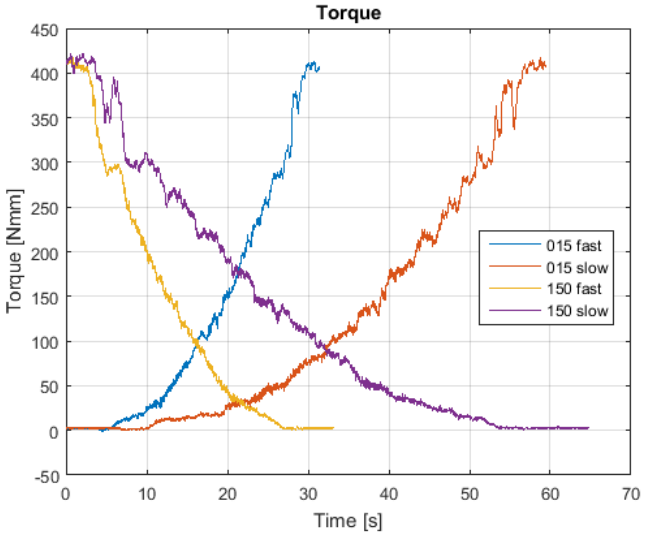

FIGURE 10.8: Torque - Continuous test - Time signal

10.4 Summary

The results form the investigation regarding the energy peak at 13 Hz discovered in Chapter 9 are not conclusive, but can be a solid base for further investigations:

- There is no relation between the energy peak and the cylinder length;
- The hypothesis of a inlet ports effect is supported by the results presented in Section 10.2, however further investigation are suggested;
- The relation between energy peak and cylinder diameter could not be investigated;
- The analysis of the torque, acquired at 2500 Hz shows evidence of effects between 5 and 15 Hz. These effects are probably caused by the combination of mechanical vibration and flow evolution in the cylinder.

Chapter 11

Conclusions

The aim of this work was to find a method to reduce the test time needed to perform experimental test to evaluate the Swirl Number and the Flow Coefficient.

At present the Swirl evaluation test is performed in a stationary way moving the inlet valves with steps of 1 mm from 15 to 1 mm. The evaluation test required around 25 minutes, but the total time needed for each cylinder head tested has to be calculated also considering the amount of time needed to move the cylinder head from the production centre to the central laboratory and the waiting list generated by the long evaluation test. Therefore if an error is found (Swirl Number outside tolerances) many cylinder heads, that in the meanwhile were produced, will need to be recalled from the market resulting in an important economic loss for Scania. Consequently the need to reduce the total time test.

The time reduction was obtained investigating the possibility of test performed with continuous valve motion. Continuous tests take less time than stationary tests and moreover are easier to be performed. Thus, it is possible to conceive the idea of performing Swirl evaluation test directly in the production chain. In this way the quality control will improve and the central laboratory can dedicates more time to Research & Development.

The project phases were:

- preliminary tests to investigate the possibility of continuous tests;
- calibration procedure to create a calibration map able to relate flow meter rotation, pressure drop over the flow meter and volume flow;
- experimental tests with continuous motion of the inlet valves;
- flow inertia study;
- LDV experimental test to investigate the flow behaviour.

In conclusion, collecting the results from all phases of the project, a continuous procedure to evaluate the Swirl Number seems to be possible.

The best setup resulting from the experimental test performed during the project is:

- Bypass valve position: 0.8;
- Valve lifter velocity: 300;
- Valve motion: cycle;
- Repetitions: at least 10 cycle.

A test with these characteristic will require about ten minutes, saving the 65% of the original time. Continuous tests with these characteristic are also easier then the standard stationary test: there is no need for the stabilisation phase, that is a very delicate phase. Therefore the continuous tests do not require the presence of a trained operator and can be at least partially automatised. These properties makes it possible to move the test to the production chain. This means that more cylinder heads can be tested and that the total time of the test for each cylinder head can be reduced even further (operating directly in the production chain will remove the time needed to bring the samples cylinder heads from the production chain to the central laboratory).

LDV tests show in both cylinder heads a Tumble motion. The spectral analysis of the axial velocity shows that there is an energy peak at 13 Hz that has higher energy content in the low Swirl cylinder head. This effect can be caused by a combination of the geometry of the intake port and the development of the Swirl inside the cylinder. However it seems to not affect the mean result of the Swirl evaluation test.

However further tests are suggested to improve even more the test time reduction and to investigate some aspects of the result of this project. Suggestions for the future test or application are made in Chapter 12.

Chapter 12

Recommendations for future work

In case of further studies or future applications of this work, some improvements and modifications are suggested.

The following suggestions are made with the purpose of improving the results and easier the experimental procedures:

- Modify the valve lifter to have equal valve lift profile for different valve velocities;
- Modify the valve lifter to be able to operate at higher speeds;
- Improve the instrumentations to acquire at higher frequency;
- Change the old counter with the new one, or a new type;
- Code a program to perform the continuous test automatically.

Having a valve lifter able to always give the same type of lift profile will improve the quality of the data and the post processing evaluation. Different lift profiles, even if scaled, cannot give the same exact result because the test time is stretched resulting in a similar total test time but with different acceleration and deceleration phases. These last two phases will influence the experimental result because the data at the same lift position are acquire for different amount of time.

The valve velocities investigated in this project were up to the maximum one allowed by the valve lifter: 40 sec/cycle. Higher valve lifter velocities can probably be used to perform Swirl evaluation tests in an even shorter time, or with higher number of repeated cycles.

LDV experimental tests have shown an energy peak around 13 Hz, this phenomenon is not visible in the other parameters because the maximum acquisition frequency was 10 Hz. Acquiring at higher acquisition frequencies will be possible to investigate the energy peak also in the other data from the rig (as done in Chapter 10 for the torque), but also will improve the accuracy of the data them self. Frequencies related to the flow behaviour higher than 13 Hz were not found, hence it is suggested to improve

the acquisition frequency of all the instruments up to 30 Hz. In the case of improved valve lifter speed it is suggested to repeat the test to understand the correct acquisition frequency, keeping in account the acquisition at 100 Hz should be avoided to exclude the mechanical vibration of the torque meter and electronic interference.

All the tests performed in this project were performed manually by the operator, by means of software inputs. Coding a computer program able to implement the procedure to perform the measure will eliminate the human error from the experimental errors (i.e. all the cycles will be equal).

During this project were used cylinder heads completely characterised and not in a development phase in order to exclude the relation between eventually strange results and unexpected behaviour of the new cylinder head. However, in case of future tests, it is suggested to tests (also) new types of cylinder heads.

Different setups, and more robust installations, can be also used to investigate more the energy peak at 13 Hz.

Bibliography

[1] Lumley John L. *Engine - an Introduction.* Cambridge University Press, 1999.

[2] Heywood John B. *Internal Combustion Engine Fundamental.* McGraw-Hill, 1988.

[3] Lindgren B. Formler för beräkning av flödesparametrar i kanalutvärderingsprogrammet "snurr". *Scania Internal Document*, Nov 2003.

[4] Swedish Standards Institute. Measurement of fluid flow by means of pressure differential devices inserted in circular cros-section conduits running full -. *Swedish Standards Institute*, Jun 2003.

[5] Dantec Dynamics. *LDA and PDA Referece Manual.* Dantec Dynamics A/S, 2011.

[6] Choong Hoon Lee Daesan Oh. Flow coefficient measurements for an engine cylinder head under transient flow conditions with continuous valve lift change. *International Journal of Engineering and Technology (IJET)*, 7(3), Jun-Jul 2015.

[7] Leistner M. Formelsammlung strömungsmessung zylinderkopf. *MAN Internal Document*, Maj 2015.